Expression levels of N-acetyltransferase 8-like (NAT8L) influence adipogenesis in brown and white adipocytes

Master Thesis

by

Helmut Josef Pelzmann, BSc

Graz University of Technology

Institute for Genomics and Bioinformatics

supervised by

Assoc.Prof. Mag.rer.nat. Dr.rer.nat. Juliane G. Bogner-Strauß

graded by

Assoc.Prof. Mag.rer.nat. Dr.rer.nat. Juliane G. Bogner-Strauß

STATUATORY DECLARATION

I declare that I have authored this thesis independently, that I have not used other than the declared sources / resources, and that I have explicitly marked all material which has been quoted either literally or by content from the used sources.

---------- ----------

Date (Helmut Pelzmann)

Acknowledgement

I am very thankful for getting the opportunity to work at the institute for Genomics and Bioinformatics in such an ambitious, professional, and friendly research group. Therefore, a special thanks to Juliane Bogner-Strauß for giving me this opportunity, supervising, and guiding my work!

Not less important, I want to thank Andreas Prokesch for sharing his knowledge with me, always taking time to discuss results, finding new ideas, and helping me with the analysis of the microarray experiments.

I think it is difficult to explain how much support, help and knowledge I got from Ariane Klatzer and Evelyn Walenta. They showed me how to correctly work in the laboratory and cell culture, and they always pushed me with new ideas! Thank you very much!

I also want to thank Florian Stöger and Thomas Schreiner for their help in the laboratory and cell culture by disburden me with some work especially in the final phase of the thesis.

At least, I want to thank all people from the institute that supported my work in any case the last months.

Not to forget, I want to thank all of my friends, who really helped me by “pulling me out” of the work and take some time to relax.

As the most important, I have to thank Franziska for her never ending patience, as my thoughts often turned around the work and she had to resign on our spare time due to my work.

Last but not least, I want to thank my parents, my grandparents, and all my family. They guided me throughout my whole life and supported every step I made. Thank you very much for providing me the basis to make this way!

Abstract

The process of adipogenesis has been extensively studied during the last several years. One approach for gaining new insights into this biological process and identifying possible new candidates is performing high-throughput analysis using microarrays. Previous experiments with mouse models showing obvious metabolic phenotypes in adipose tissues (1) revealed one transcript, N-acetyltransferase 8-like (NAT8L), which was strongly deregulated in white and brown adipose tissue of these mice. NAT8L protein (approx. 33kDa) is an enzyme that catalyzes the formation of N-acetyl-L-aspartate (NAA) from L-aspartate (L-Asp) and acetyl-CoA. The role of NAT8L as an enzyme being involved in lipid formation in brain has been previously reported (2). However, implications in adipose tissue biology have not yet been shown.

Expression profiling of mouse tissues showed that NAT8L is expressed not only in brain but also in brown (BAT) and white adipose tissue (WAT). Furthermore, NAT8L was seen to be up-regulated during adipogenic differentiation in all tested cell lines (3T3-L1, C3H/10 T1/2, immortalized brown adipose cell line - iBAC, Simpson Golabi Behmel Syndrome – SGBS cells). The highest expression of NAT8L occurred in iBACs.

To evaluate iBACs as an appropriate model for brown fat cell adipogenesis, iBACs were characterized by microarray expression analysis during differentiation. Additionally, expressions of brown fat selective marker genes as well as general adipogenic markers have been determined by qRT-PCR. It could further be shown that iBACs can be stimulated by a β-adrenergic agonist, a major physiological feature of brown fat cells. Concluding, these analyses render iBACs as a novel and *bona fide* model for *in vitro* differentiation of brown adipocytes.

Next, NAT8L expression was knocked down in iBACs. These cells did not show an obvious altered phenotype during differentiation compared to control cells and no changes in triglyceride accumulation could be observed. In contrast, l-NAT8L overexpressing iBACs showed a significant decrease in triglyceride accumulation. Furthermore, brown marker genes like C/EBPβ, PGC1α, PPARα, PRDM16, and UCP1 were up-regulated in differentiation when l-NAT8L was overexpressed in iBACs compared to control cells.

These results argue that NAT8L might play a role in brown fat differentiation and thermogenesis.

1 Abbreviations

ACSL1	long-chain-fatty-acid-CoA ligase 1 gene
AGPAT2	1-acyl-sn-glycerol-3-phosphate acyltransferase beta gene
ASPA	aspartoacylase
ATP	adenosine-5'-triphosphate
BAT	brown adipose tissue
BMI	body-mass index (kg/m^2)
BMP7	bone morphogenic protein 7
BP	biological process
BSA	bovine serum albumine
cDNA	complementary DNA
CC	cellular component
C/EBP(α,β,γ,δ)	CCAAT-enhancer-binding protein (α,β,γ,δ) (gene)
DC	direct current
DGAT (1,2)	diacylglycerol acyltransferase
ddH_2O	double distilled H_2O
DEPC	diethylpyrocarbonate
Dex	dexamethasone
DMx	differentiation medium no. x
DMEM	Dulbecco's modified eagle medium
DMSO	dimethylsulfoxide
DNA	deoxyribonucleic acid
dNTP	deoxyribonucleotide triphosphate
dsDNA	double stranded DNA
DTE	dithioerythritol
DTT	dithiothreitol
EDTA	ethylenediaminetetraacetate
ER	endoplasmatic reticulum
FA	fatty acid
FABP4	fatty acid binding protein 4 gene
FASN	fatty acid synthase gene
FBS	foetal bovine serum
FFA	free fatty acid
FM	freeze medium
GM	growth medium
HFD	high fat diet
His-Tag	codon for six histidines in a row
HRP	horseradish peroxidase

iBAC	immortalized brown adipose cell line
IBMX	3-Isobutyl-1-methylxanthine
IM	induction medium
L-Asp	L-aspartate
LPL	lipoprotein lipase gene
mRNA	messenger RNA
MOI	multiplicity of infection
NAA	N-acetyl-L-aspartate
NAT8L	N-acetyltransferase 8-like protein (gene)
ntc	non-targeting control
PBS	phosphate buffered saline
PBST	Tween including phosphate buffered saline
PCR	polymerase chain reaction
PGC-1α	PPARγ-coactivator 1α protein (gene)
PIC	protease inhibitor cocktail
PRDM16	PRD1-BF1-RIZ1 homologous domain containing 16 protein (gene)
pMSCV	plasmid murine stem cell virus
PMSF	phenylmethanesulfonylfluoride
PPARγ	peroxisome proliferator-activated receptor γ protein (gene)
P/S	penicillin/streptomycin
qRT-PCR	quantitative real-time PCR
RNA	ribonucleic acid
SGBS	Simpson-Golabi-Behmel syndrome
shRNA	short hairpin RNA
SD	standard deviation
SDS	sodium dodecyl sulfate
TBS	Tris buffered saline
TG	triglyceride
TLC	thin layer chromatography
UCP1	mitochondrial brown fat uncoupling protein 1 (gene)
WAT	white adipose tissue

2 Introduction

Since according to tradition, the problem of obesity has been known for thousands of years. As one of the first, the Indian physician Shushruta attributed massive overweight to a sedentary lifestyle which included "pampering his belly"; sleeping during the day, and being adverse to take "any sort of physical exercise". He also prescribed “physical exercise” as a way to reduce fat mass. (3)

Also Hippocrates (460-377 BC) was aware that excess food intake resulting in obesity has adverse effects on health, but excess body fat was long seen as a symbol of wealth and prosperity, as past civilizations had been faced with food-shortages and famine. (4)

Today, obesity is a rising problem not any longer linked only to high-income developed countries, since the largest increases in obesity from 1980 to 2008 have been reported for low- and middle-income countries, particularly in Latin America, North Africa, and parts of Asia. (5; 6)

Obesity, with its pre-stage adiposity, along with multiple associated morbidities is a growing social and economic burden in western society nowadays. Obesity is defined medically as a state of increased body weight, more specifically adipose tissue, of sufficient magnitude to produce adverse health effects like increasing the risk of diabetes, hypertension, heart disease, stroke, and various types of cancer. Therefore, obesity is a leading factor in increasing morbidity and mortality. The world health organization defines the body mass index (BMI) as a criterion for classification of the obesity-state. Overweight is defined by a BMI ≥25kg/m^2 and obesity is defined by a BMI ≥30kg/m^2. Although research has been focused on diet and exercise, these strategies alone do not seem sufficient in preventing obesity. In general, the biology of obesity is poorly understood and especially body weight balance is determined by genetic, environmental, and psychological factors. (5; 7)

To understand obesity, one has to face the balance of energy uptake and energy expenditure (Figure 1). While nourishment and energy storage determines the part of energy intake, physical activity, basal metabolism, and adaptive thermogenesis are the counterparts on the energy expenditure side (7).

Therefore, white adipose tissue (WAT) as the main fat/energy reservoir in humans, and brown adipose tissue (BAT), which has the function to dissipate chemical energy as heat, play an important role in the development and treatment of obesity (8; 9). While white adipocytes normally show unilocular fat accumulation and a low mitochondrial density, their brown counterparts show multilocular lipid droplets and a high number of mitochondria. With evidence that significant depots of BAT are not only present in rodents and human infants (10), but also in human adults (11), a variety of research activities have emerged on this field.

The development of white and brown adipocytes has been object of research through many years (12–14). Although brown and white adipocytes are fat cells in general, it has been

shown that they have significant differences in their gene expression patterns as well as their developmental origin. In contrast to white adipocytes, brown adipocytes share their developmental origin with myocytes, specifically cells expressing myogenic factor 5 (MYF5), a gene previously thought to be almost exclusively expressed in myogenic precursors. (8; 9; 13; 15–19).

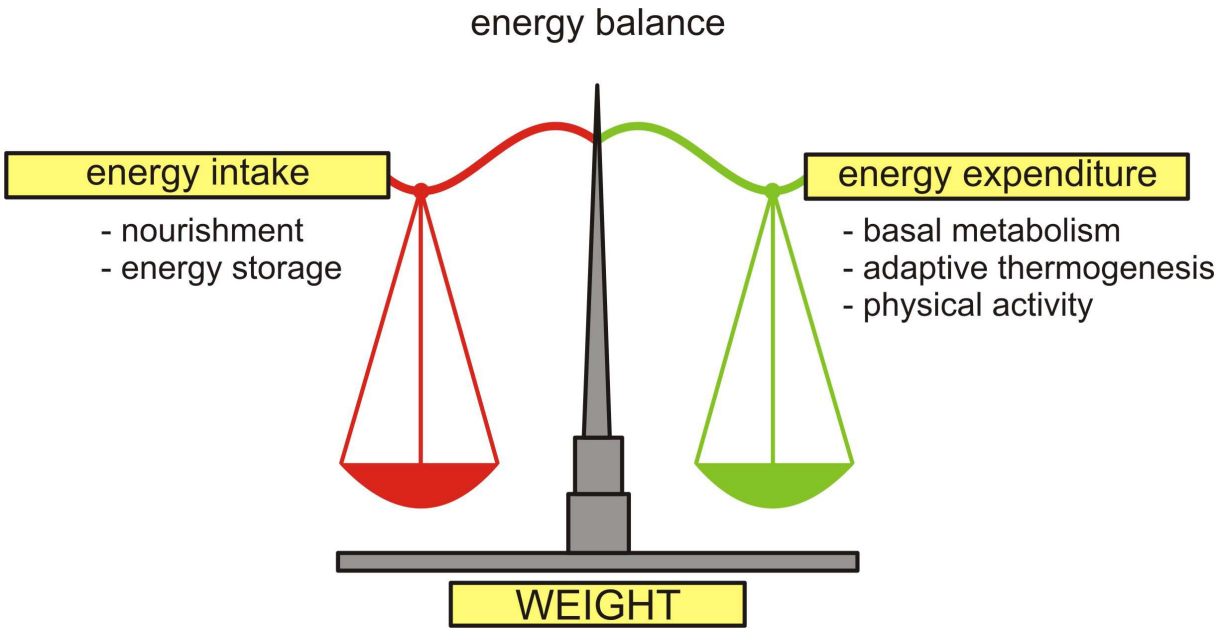

Figure 1: Key components of the energy balance system.

Brown adipocyte differentiation depends on various receptors / transcription factors that include peroxisome proliferator-activated receptor γ (PPARγ), PPARγ-coactivator-1α (PGC-1α) (20), PRD1-BF1-RIZ1 homologous domain-containing 16 (PRDM16), CCAAT/enhancer-binding protein β (C/EBPβ) (21), and bone morphogenic protein 7 (BMP7). These mediators also help establishing the thermogenic phenotype, which is essentially conferred to the expression of uncoupling protein 1 (UCP1). UCP1 is located in the inner mitochondrial membrane. Upon activation, UCP1 provides a channel for H^+ ions to reenter the mitochondrial lumen, and thereby uncoupling adenosine-5'-triphosphate (ATP) synthesis, leading to fast substrate oxidation. UCP1 activity is regulated at multiple levels. In general, BAT is activated upon cold exposure and diet-induced obesity (22). This adaption, meaning recruitment of brown-like adipocytes in WAT and/or hyperactivation of classical BAT (e.g. interscapular BAT), corresponds to β3-adrenergic stimulation determined by the sympathetic nervous system (SNS). (8; 10; 23–25)

Beside the "classical" BAT derived from myogenic precursor cells, there exist so called "recruitable brown-like" or "beige" adipocytes which can be recruited in WAT upon β3-

adrenergic stimulation (26), as mentioned above. The cellular precursor of these brown-like cells remains unknown and is now a central question for the field (Figure 2) (13).

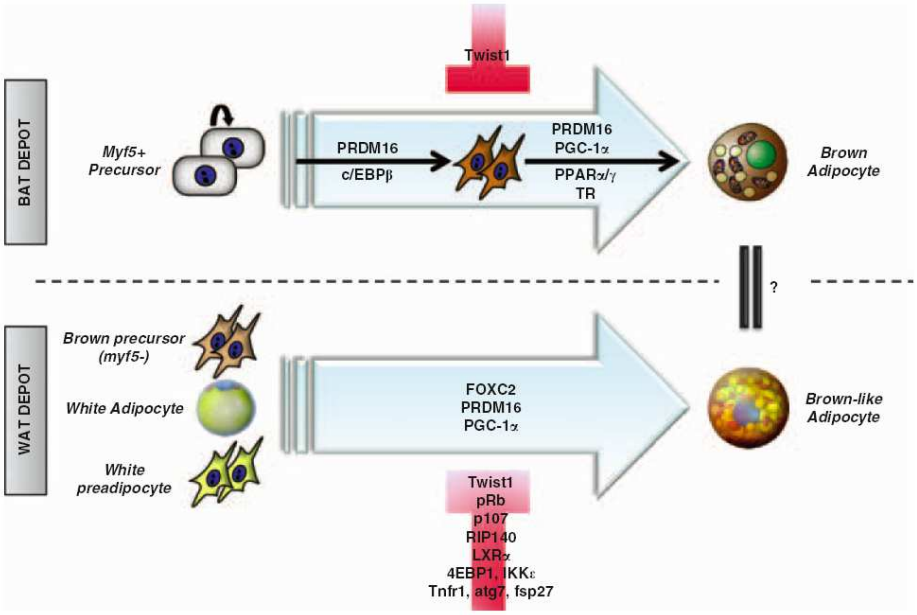

Figure 2: Brown adipocyte development in BAT and WAT depots. (13)

Although many genes involved in brown fat development, thermogenesis, and mitochondrial biogenesis have been identified, there are many connections left in this widespread network. High-throughput techniques are a useful approach to identify new candidate genes that may play a role in the process of adipogenesis. Microarray experiments with mice showing an obvious metabolic phenotype in adipose tissue (1) revealed one transcript, N-acetyltransferase 8-like (NAT8L) which was strongly deregulated in white and brown adipose tissue of these mice. NAT8L protein (approx. 33kDa) is an enzyme that catalyzes the formation of N-acetyl-L-aspartate (NAA) from L-aspartate (L-Asp) and acetyl-CoA (2; 27).

NAA is synthesized in neurons of the brain, being the second most abundant metabolite after glutamate. Furthermore, NAA has been reported to be the major source of acetyl-CoA for lipid biosynthesis in brain. In general, there are three major ways to go for acetyl-CoA in neurons. As soon as first, local energy, and second, lipid demands have been met, the synthesis of NAA via NAT8L is the third way to utilize acetyl-CoA in neurons. NAA is then translocated to oligodendrocytes for further utilization. The enzyme aspartoacylase (ASPA) is able to split NAA into L-Asp and acetyl-CoA, again. Two human inborn errors in metabolism of NAA have been reported. One is Canavan disease, in which there is an accumulation of NAA (hyperacetylaspartia) and associated spongiform leukodystrophy, due to a lack of ASPA activity. The other is a mutation of NAT8L causing a singular known human case of lack of NAA (hypoacetylaspartia). (2; 28–32)

All these facts render NAT8L an important molecule in lipid metabolism in brain. However, implications in adipose tissue biology have not yet been shown. Therefore, this thesis aims to give ideas for a possible role of NAT8L in brown and white adipogenesis.

3 Materials & Methods

3.1 Materials

3.1.1 Cell Lines

i**BAC** (SV40 T-large antigen immortalized brown adipose cell line); kind gift of Patrick Seale; University of Pennsylvania School of Medicine, Philadelphia

3T3-L1 (mouse embryonic fibroblasts; adipose like) (33; 34)

C3H/10 T1/2 (mouse embryonic fibroblasts; muscle, adipose, bone or cartilage like) (35; 36)

SGBS (human Simpson-Golabi-Behmel Syndrome cells, adipose like) (37; 38)

Cos7 (fibroblasts; recovered from green vervet monkey)

Phoenix (human embryonic kidney cell line, retroviral expression system)

3.1.2 Chemicals, reagents and buffers

- 5-(3-aminoallyl)-2´-deoxyuridine-5´-triphosphate (AA-dUTP); Sigma-Adlrich Handels GmbH
- Benzonase® Nuclease; Merck Chemicals
- Bovine Serum Albumine (BSA, Lot.Nr. K00110-1227); PAA Laboratories GmbH
- Cy-3 mono – reactive dye; VWR International (Amersham Bioscience)
- Cy-5 mono – reactive dye; VWR International (Amersham Bioscience)
- Chloroform; Sigma-Adlrich Handels GmbH
- Dimethylsulfoxide (DMSO); Sigma-Aldrich H. GmbH
- DEPC treated H_2O for molecular biology; Karl Roth GmbH + Co. KG
- Dexamethasone (Dex); Sigma-Adlrich Handels GmbH
- Diethylether; Karl Roth GmbH + Co. KG
- Dithiothreitol (DTT) 0.1M; Life Technologies, Invitrogen corp.
- Dithioerythritol (DTE); VWR International (Merck Chemicals)
- dNTP Set (100mM); Fermentas
- ECL prime; Amersham, GE Healthcare
- Ethanol absolute, for analysis; Lactan chemicals and laboratory devices
- 5x First Strand Buffer (5xFS); Life Technologies, Invitrogen corp.
- Foetal Bovine Serum (FBS, Lot.Nr. 09SB032); Lonza Inc.
- Formaldehyde; Sigma-Aldrich Handels GmbH
- Formamide; Sigma-Aldrich Handels GmbH
- Glacial acetic acid; Karl Roth GmbH + Co. KG
- Glycerol 98%; Lactan chemicals and laboratory devices
- ß-Glycerophosphate; Sigma-Aldrich Handels GmbH
- Hepes buffer 1M; Life Technologies, Invitrogen corp.

- Hexadimethrine (Polybrene 8mg/mL); Sigma-Aldrich Handels GmbH
- 3-isobutyl-1-methylxanthine (IBMX, 1g); VWR International (Merck Chemicals)
- Indomethacin crystalline (Indo); Sigma-Aldrich Handels GmbH
- Insulin (10mg/mL); Sigma-Aldrich Handels GmbH
- Isopropyl alcohol; VWR International (Fisher Scientific U.K. Ltd.)
- Isoproterenol; Sigma-Aldrich Handels GmbH
- K_2HPO_4; Sigma-Aldrich Handels GmbH
- KH_2PO_4; Sigma-Aldrich Handels GmbH
- LDS Sample Buffer 4x; Life Technologies, Invitrogen corp.
- L-Glutamine (L-Glut) 200mM; Life Technologies, Invitrogen corp.
- Lentiviral MISSION® Transmission Particles NM_001001985; Sigma-Aldrich Handels GmbH
- ß-Mercaptoethanol; Sigma Aldrich Handels Gmbh
- Metafectene; Biontex Laboratories GmbH
- Methanol Normapur for analysis; VWR International (Merck Chemicals)
- Mouse COT1-DNA; Life Technologies, Invitrogen corp.
- NaCl; Karl Roth GmbH + Co. KG
- Na_2CO_3; VWR International (Merck Chemicals)
- NaF; VWR International (Merck Chemicals)
- NaOAc; Sigma-Aldrich Handels GmbH
- Natriumorthovanadate; Sigma-Aldrich Handels GmbH
- n-hexane; Karl Roth GmbH + Co. KG
- Normocin (Normo); Eubio
- NuPAGE® Antioxidant; Life Technologies, Invitrgen corp.
- NuPAGE® 10% Bis-Tris Gel 1.0mm X 10 well; Life Technologies, Invitrogen corp.
- NuPAGE® 12% Bis-Tris Gel 1.0mm X 10 well; Life Technologies, Invitrogen corp.
- NuPAGE® 12% Bis-Tris Gel 1.0mm X 12 well; Life Technologies, Invitrogen corp.
- NuPAGE® MOPS SDS Running Buffer 20x; Life Technologies, Invitrogen corp.
- NuPAGE® MES SDS Running Buffer 20x; Life Technologies, Invitrogen corp.
- Oil Red O; ICN
- Oligo-dT Primers; Life Technologies, Invitrogen corp.
- Phosphate buffered saline (PBS, pH 7.4); Life Technologies, Invitrogen corp.
- Penicillin / Streptomycin (P/S) Sol 10.000U/mL per 10.000µg/mL; Life Technologies, Invitrogen corp.
- Poly(A)-DNA; Life Technologies, Invitrogen corp.
- Polyclonal Goat Anti-Mouse IgG / HRP, DakoCytomation

- Rabbit Polyclonal Anti-Nat8l IgG; Novus Biologicals
- Rabbit Polyclonal Anti-Ucp1 IgG; EMD Chemicals
- Protease Inhibitor Cocktail Tablets (PIC); Roche Austria GmbH
- Puromycin dihydrochloride CELL CULTURE; Sigma-Aldrich Handels GmbH
- Random Hexamer Primers 3µg/µL; Life Technologies, Invitrogen corp.
- RNaseOUT™; Life Technologies, Invitrogen corp.
- Roentogen EUKOBROM (b/w paper developer); Tetanal
- Roentogen Superfix (fixing bath for rapid processing of b/w materials); Tetanal
- Rosiglitazone Maleate (Rosi), Ebio
- 20x Saline-Sodium Citrade (SSC); Sigma-Aldrich Handels GmbH
- Seeblue® Plus2 Prestained Standard; Life Technologies, Invitrogen corp.
- Sodium Dodecylsulfate (SDS); VWR International (Merck Chemicals)
- 10% Sodium Dodecyl Sulfate (SDS), Life Technologies, Invitrogen corp.
- Super Script II Reverse Transcriptase (200U/µL); Life Technologies, Invitrogen corp.
- Super Signal West Pico Chemoluminescent Substrate; VWR International (Fisher Scientific U.K. Ltd.)
- SYBR QPCR Supermix W/Rox, Invitrogen
- TLC silica gel 60, Merck Chemicals
- 0.5% Trypsin / EDTA (10x); Life Technologies, Invitrogen corp.
- Triiodthyronine (T3); Sigma-Aldrich Handels GmbH
- Tris Glycine Buffer (TGS; 10x), Bio-Rad Laboratories GmbH
- Tris Ultra Quality, Lactan chemicals and laboratory devices
- TriZol® reagent Lot.Nr. 9848801; Life Technologies, Invitrogen corp.
- Tween, VWR International (Merck Chemicals)

3.1.3 Culture Media

Standard Growth Medium „*DMEM++++*“ (3T3-L1, C3H/10 T1/2, Cos7, Phoenix):

Dulbeccos Modified Eagle Medium (DMEM; 4,5g Glucose), Invitrogen

+ FBS 10%
+ Normocin 1:500
+ L-Glut 2mM
+ P/S 100U/mL / 100µg/mL

Differentiation Medium 1 *„DM1“* (Induction Medium, 3T3-L1):

DMEM++++

+ Insulin 2µg/mL
+ Dex 1µM
+ IBMX 0,5mM

Differentiation Medium 2 *„DM2“* (3T3-L1):

DMEM++++

+ Insulin 2µg/mL

Differentiation Medium 3 *„DM3“* (Induction Medium, C3H/10 T1/2):

DMEM++++

+ Insulin 10µg/mL
+ Dex 1µM
+ IBMX 0,5mM
+ Rosi 1µM

Differentiation Medium 4 *„DM4“* (C3H/10 T1/2):

DMEM++++

+ Insulin 10µg/mL
+ Rosi 1µM

iBAC Growth Medium *“iBAC-GM”*:

Dulbeccos Modified Eagle Medium (DMEM; 4,5g Glucose), Invitrogen

+ FBS 10%
+ HEPES 20mM
+ P/S 100U/mL / 100µg/mL

iBAC Maintenance Medium *“iBAC-MM”*:

BAT-GM

+ Insulin 20nM (1,161µL / mL-Growth Medium)
+ T3 1nM

iBAC Induction Medium *"iBAC-IM"*:

BAT-MM	
+ Dex	500nM
+ IBMX	0,5mM
+ Indo	0,125nM

Freeze Medium 1 *"FM1"* (3T3-L1, C3H/10 T1/2, Cos7, Phoenix):

DMEM++++	
DMSO	5%

iBAC Freeze Medum *"iBAC-FM"*:

BAT-GM	9%
FBS	81%
DMSO	10%

Transfection Medium *"Trans-M"* (Cos7, Phoenix):

Dulbeccos Modified Eagle Medium (DMEM; 4,5g Glucose), Invitrogen	
+ Normocin	1:500
+ L-Glut	2mM
+ P/S	100U/mL / 100µg/mL

3.1.4 Kits & devices

- 1L 0.22µm cellulose acetate (CA) Filter System; Corning Costar
- ABI Prism 7000 Sequence Detection System
- "BCA Protein Assay Kit"; VWR International (Fisher Scientific U.K. Ltd.)
- Bioanalyzer 2100, Agilent
- Coplin staining jar; Sigma-Aldrich Handels GmbH
- "Gen Elute™ Mammalian Total RNA Kit"; Sigma-Aldrich Handels GmbH
- GenPix 4000B (microarray scanner), Axon Instruments
- Hybridization chamber, Corning Costar
- Microscope cover glass; Fisher Scientific U.K. Ltd.
- Mouse cDNA Chips Nr. 20 (McC20) produced by spotting PCR products onto epoxy glass slides (Nexterion / Schott) at the bioinformatics group, Institute of Genomics and Bioinformatics, Graz University of Technology, Graz Austria
- Pressurized air duster; Fellowes (or clean in-house pressurized air)
- "RNA 6000 Nano Chips Kit"; Agilent Technologies
- Sonificator SONOPULS; Bandelin
- "QIAquick PCR Purification Kit"; Qiagen
- DNA 120 SpeedVac®, Thermo Savent

- "Triglycerides"-kit, Thermo Scientific / Fisher Diagnostics
- ULTRA TURRAX® T25 basic; IKA®-WERKE

3.1.5 qRT-PCR Primers

Table 1: Primer pairs used in human cell model.

Target gene	Forward primer	Reverse primer
l-NAT8L (E1)	TGTGCATCCGCGAGTTCCGT	CGGAAGGCCGTGTTAGGGAT
β-actin	CGCCGCATCCTCCTCTTC	GACACCGGAACCGCTCATT

Table 2: Primer pairs used in murine cell models.

Target gene	Forward primer	Reverse primer
C/EBPβ	GGACTTGATGCAATCCGGA	AACCCCGCAGGAACATCTTTA
FABP4 / AP2	CGACAGGAAGGTGAAGAGCATC	ACCACCAGCTTGTCACCATCTC
l-NAT8L (E1)	TGTGCATCCGCGAGTTCCGC	GCGGAAAGCCGTGTTGGGGA
s-NAT8L (I1-E2)	CACCTGCCACCTCACCTGTGCC	GGCCAGAATCACCTTGCGGCT
NAT8L (I2-3)	TGTGCGCTGCACACGGACAT	GCCCACAACGTTGCCGTCCA
PGC-1α	TCTCTGGAACTGCAGGCCTAAC	TCAGCTTTGGCGAAGCCTT
PPARα	CCTGAACATCGAGTGTCGAATATG	GCGAATTGCATTGTGTGACATC
PPARγ2	TGCCTATGAGCACTTCACAAGAAAT	CGAAGTTGGTGGGCCAGAA
PRDM16	TCCACAGCACGGTGAAGCCA	ATCTGCGTCCTGCAGTCGGC
TFIIβ	GTCACATGTCCGAATCATCCA	TCAATAACTCGGTCCCCTACAA
UCP1	ACACCTGCCTCTCTCGGAAA	TAGGCTGCCCAATGAACACT

3.1.6 Thin layer chromatography (TLC) reagents and buffers

Protein lysis buffer	NaOH	0.3N
	SDS	0.1%

3.1.7 µArray reagents and buffers

3.1.7.1 Aminoallyl labeling of RNA for Mouse cDNA Chips (McC)

Phosphate buffers

1M phosphate buffer (KPO_4, pH 8.5-8.7):

1M K_2HPO_4	9.5mL
1M KH_2PO_4	0.5mL

Phosphate wash buffer (5mM KPO_4, pH 8.0, 80%, buffer will be slightly cloudy)

1M KPO_4 pH 8.5	0.5mL
MilliQ water	15.25mL
95% ethanol	84.25mL

Aminoallyl dUTP

For a final concentration of 100mM add 19.1µL of 0.1M KPO_4 buffer (pH 7.5) to a stock vial containing 1mg of aa-dUTP. Gently vortex to mix and transfer the aa-dUTP solution into a new microfuge tube. Store at -20°C.

Labeling mix (50x) with 3:2 aa-dUTP:dTTP ratio

		final concentration
dATP (100mM)	5µL	(25mM)
dCTP (100mM)	5µL	(25mM)
dGTP (100mM)	5µL	(25mM)
dTTP (100mM)	3µL	(15mM)
aa-dUTP (100mM)	2µL	(10mM)

Store at -20°C.

Sodium carbonate buffer (Na_2CO_3, 1M, pH 9.0)

Dissolve 10.8g Na_2CO_3 in 80mL of MilliQ water and adjust pH to 9.0 with 12 N HCl (approx. 15mL of 25% HCl) and bring volume up to 100mL with MilliQ water. Dilute 1:10 with water for the dye coupling reaction. Store at room temperature, use within one month.

Cy-dye esters

Cy3-ester and Cy-ester are provided as a dried product. Resuspend a tube of dye ester in 73µL DMSO before use. Wrap all reaction tubes with foil and keep covered as much as possible in order to prevent photobleaching of the dyes. If not used immediately dye esters must be aliquoted and stored at -80°C. Any introduced water will result in a lower coupling efficiency due to the hydrolysis of the dye esters. Since DMSO is hygroscopic (absorbs water from the atmosphere) store it well sealed in desiccant.

NaOAc (100mM)

Mix 0.5mL 3M NaOAc with 14.5mL MilliQ water to get 100mM NaOAc.

3.1.7.2 Mouse cDNA Chip (McC) probe hybridization

Prehybridization buffer

To make 500mL prehybridization buffer combine:

volume percentage	volume	starting material	end concentration
25%	125mL	20x SSC	5x SSC
1%	5mL	10% SDS	0.1% SDS
	5g	BSA	1% BSA
74%	370mL	MilliQ water	

Filter through 0.22mm filter.

1x hybridization buffer

To make 1mL hybridization buffer combine:

volume percentage	volume	starting material	end concentration
50%	500µL	99.5% Formamide	50% Formamide
25%	250µL	20x SSC	5x SSC
1%	10µL	10% SDS	0.1% SDS
24%	240µL	MilliQ water	

Wash buffer I (low stringency buffer)

To make 1L wash buffer I combine:

volume percentage	volume	starting material	end concentration
10%	100mL	20x SSC	2x SSC
1%	10mL	10% SDS	0.1% SDS
89%	890mL	MilliQ water	

Wash buffer II (low stringency buffer)

To make 1L wash buffer II combine:

volume percentage	volume	starting material	end concentration
5%	50mL	20x SSC	1x SSC
95%	950mL	MilliQ water	

Wash buffer III (high stringency buffer)

volume percentage	volume	starting material	end concentration
2.5%	25mL	20x SSC	0.5x SSC
97.5%	975mL	MilliQ water	

3.1.8 Western Blot reagents and buffers

Blocking solution (NAT8L antibody)

PBST
+5% BSA

Blocking solution (UCP1 antibody)

TBST
5% BSA

Lysis buffer	aqua biodestillata ster. “Fresenius”, Fresenius	
	+ 10%	glycerol v/v
	+ 10mM	ß-glycerophosphate
	+ 10mM	NaF
	+ 100µM	Natriumorthovanadate
	+ 2.5%	SDS v/v
	+ 50mM	Tris-HCL
PBST buffer	PBS	
	+ 0.05%	Tween

Tris buffered saline (TBS) 10x, pH 7.5

	MilliQ water	
	+ 10mM	Tris
	+ 150mM	NaCl
TBST buffer	1x	TBS
	+ 0.1%	Tween

Transfer buffer

volume percentage	volume	starting material	end concentration
10%	100mL	10x TGS buffer	1x TGS buffer
20%	200mL	Methanol	
70%	700mL	MilliQ water	

3.1.8.1 Antibody solutions

NAT8L antibody was diluted 1:1000 in PBST buffer containing 5%BSA.
UCP1 antibody was diluted in 1:750 in TBST buffer containing 1% BSA.
Anti rabbit antibody was diluted 1:9000 in PBST for NAT8L antibody and 1:2000 in TBST containing 1%BSA for UCP1 antibody.

3.2 Methods

3.2.1 Cell culture

3.2.1.1 Handling

- Storage

  For long-term storage, cells were held deep frozen in liquid nitrogen tanks. Cells were frozen in special Freeze Media (FM1 and iBAC-FM) to avoid cell death.

  For thawing, the frozen cells had to be diluted very fast in a ratio of about 1:10 with fresh, preheated media. 24h after the cell settlement the media was changed.

- Cultivation

  3T3-L1, C3H/10 T1/2, Cos7, and Phoenix cells were cultivated in DMEM++++ and iBACs in iBAC-GM. The change of media was done latest every 3 days if splitting was not necessary.

- Splitting

  To avoid total cell confluence, which is especially important for the 3T3-L1, C3H/10 T1/2, and iBAC cell lines, they have to be split at 60-80% of confluence to keep full differentiation capacity. Therefore the medium was removed, the cells were washed with PBS twice, and trypsin solution was added (1mL for a 75cm^2 growth plate) to disconnect the dish-cell interaction. Either DMEM++++ or iBAC-GM was used to stop the reaction and to seed the cells into the appropriate dishes.

- Freeze cells for long-term storage

  For long-term storage, cultured cells had to be frozen again. Therefore, the medium was removed, the cells were washed with PBS twice and trypsin solution was added (1mL for a 75cm^2 growth plate). After disconnection, either DMEM++++ or iBAC-GM was used to stop the reaction and solute the cells in medium. Soluted cells were centrifuged (5min, 1200rpm). After centrifugation the pellet was dissolved in either FM1 or iBAC-FM and aliquoted to “Cryo-Tubes” each 1mL.

3.2.1.2 Differentiation

3T3-L1 cells were grown to confluence (day -2) and induced to differentiate using the standard hormonal cocktail, DM1, on day 0. The media was changed to DM2 on day 3, to DMEM++++ on day 5, and from then on every 2 days.

C3H/10 T1/2 cells were grown to confluence (day -2) and induced to differentiate using the DM3 cocktail (adipose like standard cocktail for these cells) on day 0. The media was changed to DM4 on day 3 and from then every 2 days.

iBACs were examined for their ability to differentiate in different states of confluence. It could be shown that cells differentiate from 90% to 2 days after confluence. The best results were obtained when cells were induced to differentiation at 100% confluence with iBAC-IM (day 0). The medium was changed to iBAC-MM after 48h, at day 4, and then every day.

3.2.1.3 β3-adrenergic stimulation (Isoproterenol)

The influence of Isoproterenol boosts on iBAC gene expression has been reviewed during differentiation with qRT-PCR. Therefore, medium had to be changed to iBAC-MM 2h before stimulation with 10µM Isoproterenol (at the final concentration). Stimulation was carried out for 4h.

3.2.1.4 Transfection

To transiently integrate foreign DNA into Phoenix cells, the plasmids were transfected using metafectene. This transfection reagent changes the DNAs to compact structures to ensure the easy entry into the cell, and, in addition, destabilizes the lipid membrane coating the DNA/RNA by repulsive electrostatic forces to provide it in better accessible conditions.
One hour before transfection, the standard medium DMEM++++ had to be changed to Trans-M. For each 6-well, 1µg DNA and 4.5 µL metafectene / µg DNA were added to 50µL Trans-M each and were mixed together gently. For negative controls, an empty vector was transfected. After 20 minutes of rest, the metafectene-DNA cocktails were pipetted dropwise into the growth media over the cells (not directly on the cells!). The medium was changed to DMEM++++ after 4h and the maximum expression was reached after 48-72h.
The transfection of the Phoenix cells with pMSCVpuro, *and* pMSCV-l-NAT8L led to amphotrophic lentiviral particles in the supernatant, which were collected and used further on for transduction.

3.2.1.5 Transduction

The common procedure to stably integrate foreign DNA into the genomic DNA of 3T3-L1 and iBACs is transduction using lentiviral particles as carriers.

- **Silencing of NAT8L in 3T3-L1 cells**

  For stable silencing of NAT8L, 3T3-L1 cells were seeded into 6-well plates and transduction was started at about 30-40% confluence with infection with 150,000 or 300,000MOI per well (MOI …multiplicity of infection) of shRNA lentiviral particles and non targeting control (shNTC). This equals approx. 4-6 MOI per cell. To increase the efficiency of retroviral infection, polybrene (6µg/mL at the final concentration) was

added to the medium. Polybrene is a polycation that neutralizes the charge interactions between the pseudoviral capsid and the sialic acid of the cellular membrane. As excessive exposure of polybrene can be toxic to cells, the media had to be changed after an overnight incubation (16-24h). For stable selection, puromycin was added to the medium in a final concentration of 3µg/mL for at least 5 to 6 days. After the death of non-transduced cells, the remaining 3T3-L1 cells were transferred to a 75cm^2-flask with fresh DMEM++++. During the whole selection process cells must not get more than 80% confluent.

- **Overexpression and silencing of NAT8L in iBACs by the use of single cell selection**

  iBACs were seeded into 6 well plates and transduction was started at about 30-40% confluence. To increase the efficiency of retroviral infection, polybrene (8µg/mL at the final concentration) was added to the iBAC-GM.

  To achieve stable overexpression of l-NAT8L in these cells, 1mL of the lentiviral particles containing supernatant from transfected phoenix cells mixed with 1ml of iBAC-GM was used for transduction. If used directly from Phoenix cells, the supernatant must be centrifuged 5 minutes at 1200rpm removing eventually existing Phoenix cells before infection.

  For stable silencing of NAT8L, iBACs were infected with 150,000 or 300,000MOI per well of shRNA lentiviral particles. This equals approx. 2-4 MOI per cell.

  Due to puromycin resistance of iBACs (about 1/3 survives puromycin selection in a 75cm^2-flask) three selection steps were applied:

  - First, puromycin was added to the media in a final concentration of 30µg/mL for each well until cells needed to be split before becoming confluent.
  - Second, cells were disseminated as thin as possible into a 6cm dish for single cell selection. After about 12h, single cells were picked up under the microscope with a 10µL pipette and transferred to a 24 well plate with fresh iBAC-GM (carefully draw off / scrape off the cells from the bottom of the dish).
  - Third, puromycin was added a second time into the media of each well where cells were found for final selection.

  After the death of non-transduced cells, the remaining iBACs were transferred to a 25cm^2-flask with fresh iBAC-GM. Final evidence if the selection process worked was given by qRT-PCR analysis of l-NAT8L expression levels.

3.2.2 RNA-Isolation

3.2.2.1 Cell culture cells

For **qRT-PCR analysis,** cells were washed with PBS twice and the "Gen Elute™ Mammalian Total RNA Miniprep Kit" was used for RNA isolation. In contrary to the kit-directions, the column bound RNA was resuspended in 40µL DEPC treated H_2O for 1min, centrifuged for 1min at 16.000g and eluted again with the same solution by centrifugation.

For **microarray experiments,** iBACs in 75cm^2-flasks were also washed with PBS twice and then harvested using TriZol® reagent (3mL for each flask). If the samples were frozen at -80℃, they had to thaw at room temperature for 30min and afterwards samples were chloroformed with 0.2mL per each mL TriZol® reagent to separate RNA, DNA, and protein phases. After roughly mixing for 15-20s and calm down for 2-3min at room temperature, the samples were centrifuged at 4℃ and 12,000g for 17min. After centrifugation 3 phases were discernable. The colorless phase on the top contains RNA and has to be pipetted off very cautiously into a new collection tube. The white phase is the one with proteins and the red colored one indicates DNA. After adding 0,5mL isopropyl alcohol per each mL TriZol® reagent, the samples were vortexed, incubated at room temperature for 10min, and then centrifuged at 4℃ and 12,000g for 20min. The supernatant was discarded and 1mL ethanol (75%) was added per each mL TriZol® reagent. Subsequently the samples were vortexed and centrifuged at 4℃ and 7,500g for 6min. The supernatant was discarded and the residual pellets were dried depending on the size (5-30min). The RNA was suspended with DEPC treated H_2O depending on the expected amount of RNA (as less volume as possible since the RNA is needed in a very high concentration).

3.2.2.2 Mouse Tissue

For homogenization with ULTRA TURRAX®, 1mL TriZol® reagent per 100mg mouse tissue sample was added (1,5mL per 100mg for WAT-samples). To avoid overheating, the tubes were kept on ice. The homogenized samples were incubated at room temperature for 5min and afterwards samples were chloroformed with 0,2mL per each mL TriZol® reagent to separate RNA, DNA, and protein phases. After roughly mixing for 15-20s and calm down for 2-3min at room temperature, the samples were centrifuged at 4℃ and 12,000g for 19min. After centrifugation 3 phases were discernable. The colorless phase on the top contains RNA and has to be pipetted off very cautiously into a new collection tube. After adding 0,5mL isopropyl alcohol per each mL TriZol® reagent, the samples were vortexed, incubated at room temperature for 10min and then centrifuged at 4℃ and 12,000g for 10 min. The supernatant was discarded and 1mL ethanol (75%) was added per each mL TriZol® reagent.

Subsequently, the samples were vortexed and centrifuged at 4℃ and 7,500g for 5min. The supernatant was discarded and the residual pellets were dried depending on the size (5-30min). The RNA was suspended with DEPC treated H_2O depending on the expected amount of RNA (as less volume as possible since it is better to have the RNA in a high concentration for further use in cDNA synthesis).

In both cases the RNA concentration was measured by NanoDrop spectrophotometer and the samples were stored at -80℃.

3.2.3 cDNA synthesis

1µg of RNA, 1µL each Oligo-dT Primers, dNTP-mix, and 300ng/µL Random Primers were filled up to 12µL with DEPC treated H_2O, heated to 65℃ for 5 minutes to destroy the secondary structure and subsequently chilled on ice for the same time. After addition of 4µL 5xFS, 2µL 0,1M DTT, and 1µL RNase Out, the samples were gently mixed and incubated at 37℃ for 2min. 1µL of the reverse transcriptase "SuperScript II" was added and the samples were incubated at 25℃ for 10 min and subsequently at 42℃ for 50min in the water bath. The reactions were inactivated at 70℃ for 15min and afterwards stored at -20℃.
For qRT-PCR analysis cDNA had to be diluted to a final concentration of 1ng/µL.

3.2.4 qRT-PCR

The polymerase chain reaction (PCR) allows amplifying of exactly defined DNA sequences up to 3kbp, with special polymerases even up to 40kbp. Quantification of these sequences (qRT-PCR) requires a fluorescent, in this case SYBR-green. SYBR-green absorbs blue light at a maximum wavelength of 498nm and emits green light at a maximum wavelength of 522nm when bound to double stranded DNA (dsDNA). Fluorescence increases proportionally to the formatted dsDNA amount. It has to be said that the DNA quantification works correctly only during the exponential production. Housekeeping genes murine TFIIβ and human β-actin were used as reference.
For each qRT-PCR run we used 4.5ng cDNA solved in 4.5µL ddH_2O, 4.5µL of 800nM Primers, and 9µL SYBR green.

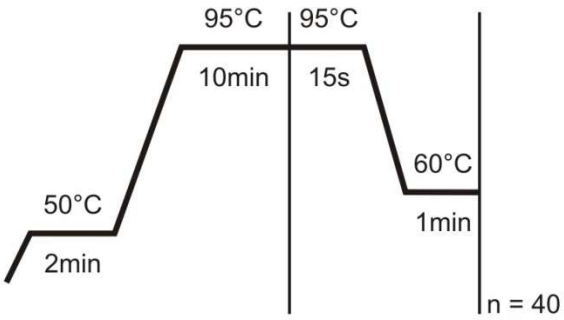

Figure 3: Temperature program for qRT-PCR.

3.2.5 Thin layer chromatography (TLC)

For analysis of lipids with TLC, cells were grown in 6-well plates. Cells were washed twice with PBS. Lipids were harvested by incubating sample cells with 1mL hexane/isopropyl alcohol (3:2) per well for 10 minutes on the shaker, transferred into a “Pyrex”-tube, and stored at -20°C. “Pyrex”-tubes had to be enclosed w ith “ParaFilm” because of the fugacity of the solvent. For protein harvesting, 500µL of protein lysis buffer (see 3.1.6) were added per well and the cells were lysed for 3-6h on the shaker. The lysate was transferred into a 1.5mL tube and stored at -20°C.

Protein samples were quantified using the “BCA Protein Assay Kit”, Pierce.

On the basis of the protein samples, the proper amount of lipids was calculated and used for TLC. Lipid samples were dried with SpeedVac® (approx. 20min). Meanwhile, the TLC-chamber, mobile phase (n-hexane : diethyl ether : glacial acetic acid – 70 : 29 : 1), and the TLC plate (TLC silica gel 60, Merck Chemicals) has been prepared in the hood. Filter paper had to be used for saturation of the chamber. Dried samples were resolved in 30µL chloroform and applied to one TLC plate for two times. The matrix was placed inside the chamber so, that filter paper and matrix did not touch. TLC was run with two TLC plates. The first run was just with the mobile phase mentioned above, but for the second run toluol was used as an additional mobile phase. After TLC plates were dried and incubated with $CuSO_4$ (dried again), they had to be “baked” for 12min at 130°C.

3.2.6 µArray

For µArray analysis, cells were grown to confluence, induced, and differentiated (see 3.2.1.2) for 7 days. RNA was harvested on day 0, day 3, and day 7 of differentiation (see 3.2.2.1).

3.2.6.1 Quality control of RNA Agilent 2100 Bioanalyzer

RNA quality control for µArray analysis was done with the "RNA 6000 Nano Chips Kit".

3.2.6.2 Aminoallyl labeling of RNA for Mouse cDNA Chips (McC)

Aminoallyl labeling

To 20µg of total purified RNA, 2µL random hexamer primers (3mg/mL) were added and the final volume was brought up to 18.5µL with DEPC treated H_2O. After incubating at 70°C for 10min, the samples were snap-frozen in ice for 30s, and briefly centrifuged at >10,000rpm. 6µL 5x FS buffer, 3µL 0.1M DTT, 0.6µL 50x aminoallyl-dNTP mix, and 2µL SS II RT (200U/µL) were added. Samples were mixed and incubated over night at 42°C in the water quench.

The samples were briefly centrifuged at >10,000rpm before and after all following steps. To hydrolyze RNA, 10µL 1M NaOH, and 10µL 0.5M EDTA were added, samples were mixed and incubated at 65°C for 15min. To neutralize pH, 10µL of 1M HCl were added.

Reaction purification I (removal of unincorporated aa-dUTP and free amines)

Qiagen "QIAquick purification kit" was used with a modified protocol because some of the Qiagen supplied buffers contain free amines which compete with the Cy dye coupling reaction.

cDNA samples were mixed with 300µL (5x reaction volume) buffer PB (Qiagen supplied) and transferred to a QIAquick column. The column was transferred into a 2mL collection tube (Qiagen supplied) and centrifuged at ~13,000rpm for 1min. After discarding the flow through, reactions were washed twice with 750µL phosphate wash buffer and centrifuged at ~13,000rpm for 1min. Again the flow through was discarded and the column was centrifuged for one additional minute at 13,000rpm. After transferring the column to a new 1.5mL collection tube, 30µL phosphate elution buffer were carefully added to the center of the column and incubated for 1min at room temperature. Samples were eluted twice by centrifugation at 13,000rpm for 1 minute, so that the final volume was ~60µL. Samples were dried in a SpeedVac® with 45 minutes run time and 30 minutes heating time.

Coupling aa-cDNA to Cy dye ester

Aminoallyl-labeled cDNA had to be resuspended in 4.5µL 0.1M sodium carbonate buffer (Na_2CO_3, pH 9.0) and 4.5µL of the appropriate NHS-ester Cy dye (prepared in DMSO) were added. Cy dyes have been wrapped in foil and sequestered from light as much as possible. The reaction was incubated for 1h in the dark at room temperature.

Reaction purification II (removal of uncoupled dye)

The second purification step was done with the Qiagen "PCR Purification Kit" (modified protocol). Therefore, first 35µL of a 100mM NaOAc (pH 5.2), and then 250µL (5x reaction volume) buffer PB (Qiagen supplied), were added. Samples were applied to a column in a 2mL collection tube (Qiagen supplied) and centrifuged at 13,000rpm for 1min. To wash, 750µL of buffer PE (Qiagen supplied; ethanol has been added before use) were added and the column was centrifuged at 13,000rpm for 1 minute. Flow through was discarded and the column was centrifuged for an additional minute like before (the column should have the color of the dye now). The column was now transferred to a new 1.5mL collection tube and 30µL of buffer EB (Qiagen supplied) were carefully added to the column membrane. After 1min incubation at room temperature, samples were eluted by centrifugation at 13,000g for 1min for two times (final volume again 60µL; the solution should have the color of the dye).

Finally Cy3 and Cy5 probes were dried with SpeedVac® (45 minutes running time, 30 minutes medium heating time) and procedure was continued with hybridization.

3.2.6.3 Mouse cDNA Chip (McC) probe hybridization

Prehybridization

Prehybridization buffer had to be prepared (see 3.1.7.2), sterilized by filtration using an acrylic copolymer filter (Corning; pore size 0.45µm), and preheated at 42℃ (water quench) for ~30 minutes before use. The printed slide(s) were placed in a Coplin jar containing preheated prehybridization buffer and incubated at 42℃ (water quench) for 45 minutes.

Washing slides:

- Five Coplin jars were filled with MilliQ water and one with isopropyl alcohol.
- Slides were dipped five times into every Coplin jar (grab slides always at the labeled end).
- The Coplin jar with isopropyl alcohol was used for the last washing step.
- Water has been changed every two slides.

- Slides were dried by immediate centrifugation at 1,500rpm for 2min.

Slides were used immediately for ensuring optimal hybridization efficiency.

Hybridization

1x hybridization buffer was used for hybridization (see 3.1.7.2). Cy3 samples were resuspended with 24µL of 1x hybridization buffer. The suspension was transferred to the Cy5 samples and mixed gently. To block nonspecific hybridization, 1µL of each COT1-DNA (20µg/µL), and Poly(A)-DNA (20µg/µL) were added to the probes. Probe mixtures were heated at 95℃ for 3 minutes and snap cooled on ice for 30 seconds for denaturation. After centrifugation at the 13,000rpm for 1 minute, probe mixtures were kept at room temperature and used immediately.

To apply the labeled probe mixture, a prehybridized microarray slide (array side up) was placed between the guide teeth in the bottom half of the hybridization chamber. The labeled probe mixture (~26µL) was pipette to the slide surface near one end of the array print area (avoid bubbles). A 22mm x 60mm microscope glass coverslip was dusted off with compressed air and very cautiously placed on the arrays surface so that the cDNA pool was dispensed all over the array area without bubbles. If necessary, the position of the coverslip glass was carefully adjusted, so that there was an even margin between the edge of the coverslip and the edge of the slide. 10µL ddH_2O had to be added to the small wells at each end of the chamber, the chamber was covered, sealed with clamps, wrapped in foil (light-tight), and incubated in the water quench at a temperature of 42℃ for 16-20h. The hybritization chamber must be stored horizontally and never flipped; this may cause the cover slip to shift from the slide and adversely affect the hybridization.

Washing slides after hybridization

Wash buffer I, II, and III were prepared (see 3.1.7.2) and preheated to 30℃ (in the water quench) before usage. One Coplin jar filled with wash buffer I was also preheated to 42℃ in another water quench. The hybridized slide should be exposed to light as little as possible so during all washing steps the slide was kept covered. The transfer time between the wash solutions was kept as short as possible to not dry out the slides during the washing procedures.

After incubation the foil was removed, the hybridization chamber was unsealed carefully, and the coverslip was removed by submerging the slide into the Coplin jar filled with wash buffer I for 2 minutes. After the coverslip had been removed, the slide was placed in a staining dish

and consecutively washed with wash buffers I, II and III while agitated 5 minutes at room temperature step.

After drying slides by final immediate centrifugation at 1,500rpm for 2 minutes, slides had been stored in a light tight slide box until they were scanned.

3.2.6.4 Scanning slides with GenePix 4000B

Every microarray slide was scanned with GenePix 4000B (Axon Instruments) using the software package "GenePix Pro 4.1". Two scans, a high gain scan and a low gain scan, were performed for each slide for measurement range extension. The two color-channel gains had to be adjusted for each scan, so that Cy3 and Cy5 color intensities were equal for each scan.

3.2.6.5 Analysis

Analysis of microarray data was done according to a standard process (Figure 4). Preprocessing (high / low scan, filtering) was done using the GenePix Pro 4.1 software. Merging of high and low scan was done with an in-house PEARL script provided by Andreas Prokesch, PhD (Institute for Genomics and Bioinformatics; Graz University of Technology). Within-array normalization (Print-tip LOWESS) (39; 40) and between-array normalization was performed with "CARMAweb 1.5" (41) (no background correction). Gene set restriction and clustering was done with Genesis 1.6.0 (42). Finally, the "DAVID Functional Annotation Tool" (43; 44) was used for GO annotation and enrichment analysis.

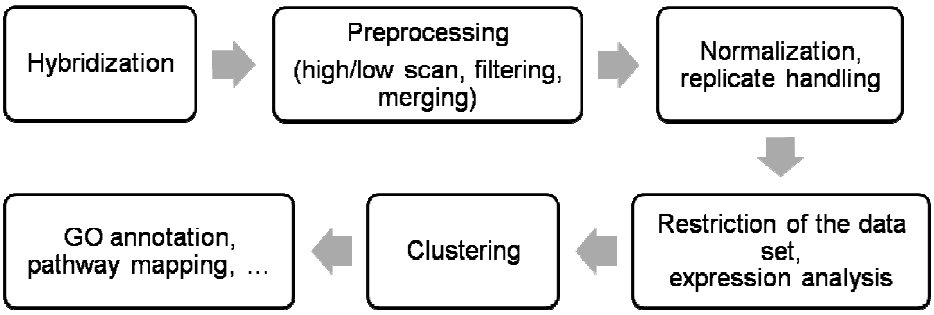

Figure 4: standard microarray workflow.

3.2.7 Oil Red O staining

The cells were washed with PBS twice and subsequently fixed with formaldehyde (10%) for 30min. The Oil Red O stock (0.25g Oil Red O powder diluted in 50mL isopropyl alcohol) is ready for use when diluted with ddH_2O (3:2) and filtrated through filter paper (1, Ø 110mm). After sucking off the formaldehyde, the Oil Red O dye was pipetted onto the cells and incubated for 30min. The fixed and dyed cells were stored covered with ddH_2O.

3.2.8 Protein quantification

Protein quantification was done with the “BCA Protein Assay Kit”, Pierce.

3.2.9 Triglyceride quantification

Triglyceride (TG) quantification was done with “Triglycerides”-kit, Thermo Scientific / Fisher Diagnostics.

3.2.10 Western Blot

A benzonase digest was done to achieve an easier handling of the samples. For this purpose, the protein solutions were inactivated at 95°C for 5 minutes and subsequently chilled back to room temperature. After the addition of 1µL benzonase, the samples were incubated at room temperature for 1h and centrifuged for 3min at 13,000g. If there had been a visible pellet after centrifugation, a separation of the supernatant would have been necessary.

3.2.10.1 Gel electrophoresis

To separate proteins because of their different charge and size, a gel electrophoresis was done. For this purpose, 40-70µg proteins, collected as mentioned before, were used. The Bio-Rad western blot chamber was filled with the gels and 700mL of the diluted NuPAGE® buffer (1x). Before loading, 500µL antioxidant was pipetted (dropwise) over the gel slots. The samples, containing the proteins, 8µL 4x LDS, and 1µL DTE were filled up to 35µL with H_2O sterile, mixed, incubated for 10min at 70°C to dena turize the proteins, and transferred into the gel slots. As a standard 10µL of Seeblue® Plus2 mixed with 20µL sterile H_2O and 5µL 4x LDS was used.
At least the gel was run for about 1h at 175V (DC), depending on the distribution of proteins that should be achieved.

3.2.10.2 Transfer

In order to make proteins accessible to antibody detection, they are moved from the gel onto a membrane (nitrocellulose). The proteins in the gel have a negative net charge, so they can be blotted on the membrane via an electric field.
The membrane was activated in ddH_2O for ~5 minutes. Afterwards filter papers, membrane, gel, and sponges were sucked with transfer buffer, arranged in a clamping tool, and fixed (Figure 5). This transfer plate tool was transferred into the transfer chamber, which was filled up with transfer buffer and an ice block. The transfer was done for 1.5h at 130-170V.

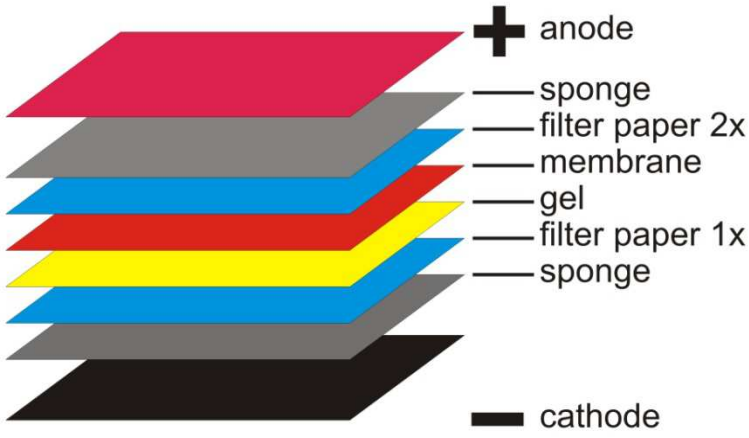

Figure 5: Transfer assembly for western blot.

To prevent the antibodies from binding to the membrane instead of the antigen, the membrane was blocked for 1h in a blocking solution specific to the antibody used (see 3.1.8)

3.2.10.3 Incubation

The membrane was incubated with two antibodies. The first one, which binds selectively to the target protein, was incubated at 4℃ over night on the 360° rotator. After a triple wash with either PBST for the NAT8L antibody or TBST for UCP1 antibody, the second antibody, anti rabbit, was added and the blot was incubated at room temperature for 2h on the 360° slide. Finally, the membrane was washed three times with the appropriate buffer again.

3.2.10.4 Exposure

Either 500µL of each of the “Amersham ECL prime” solutions or 1mL of each of the “Super Signal West Pico” solutions were mixed, pipetted onto the membrane, and incubated for 5 minutes. To avoid drying of the membrane, it was kept in a cling film for the rest of the handling. The enhanced chemoluminescence of the antibodies hit the photo paper (exposure time depending on intensity), which was developed with Roentogen EUKOBROM and Roentogen Superfix and finally washed with ddH_2O.

3.2.11 Statistics

Average and standard deviation (SD) for qRT-PCR results were calculated from three biological replicates. If the data shown stems from one representative experiment, the SD was calculated from technical replicates. Significance levels were set at *$p < 0.05$, **$p < 0.01$, and ***$p < 0.001$.

4 Results

4.1 Investigation of NAT8L gene and protein structure

In human, the NAT8L gene (official name: “NAT8L N-acetyltransferase 8-like (GCN5-related, putative)” [*Homo sapiens*], gene ID: 339983)[1] is located on chromosome 4 (4p16.3). As all experiments have been carried out with murine models, all further use of “*Nat8l* gene” points on “NAT8L N-acetyltransferase 8-like [*Mus musculus*]” (gene ID: 269642)[2] located on chromosome 5 (5 B2; 5) of the mouse genome.

Two transcripts have been reported for the human NAT8L gene[3], but until now just one transcript was known for the murine homologue[4]. In human, two proteins containing 302aa (~33kDa) and 134aa (~15kDa) are known, while in mouse, three proteins are reported (299aa / ~33kDa, 134aa / ~15kDa, 53aa / ~6kDa). All further use of l-NAT8L points on the longest mRNA / ~33kDa protein and all use of s-NAT8L points on the shorter mRNA / ~15kDa protein.

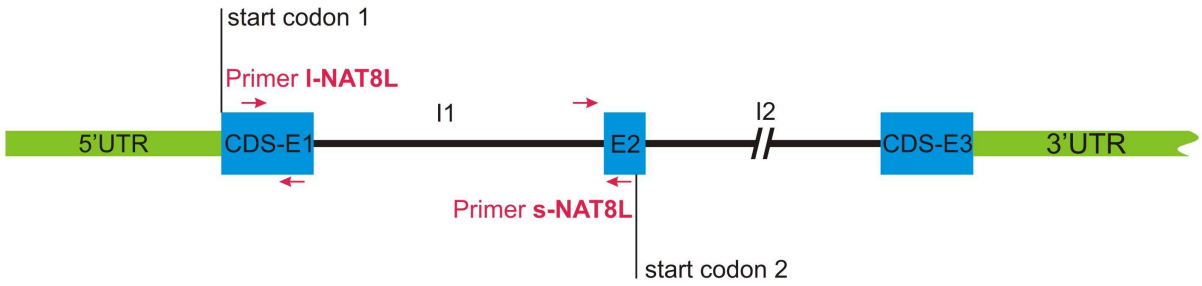

Figure 6: NAT8L gene structure. Coding sequence (CDS) indicated in blue. Untranslated regions highlighted in green. Primer locations indicated by red arrows.

Primers for l-NAT8L have been designed with an amplicon located in exon 1. With the assumption that a second transcript exists also in mice, primers have been designed to detect s-NAT8L. The primers bind to a possible 5’UTR of s-NAT8L. For detailed gene structure see Figure 6. As the N-acetyltransferase activity has just been reported for the 33kDa protein, all overexpression and silencing experiments were carried out with focus on l-NAT8L.

[1] http://www.ncbi.nlm.nih.gov/gene/339983
[2] http://www.ncbi.nlm.nih.gov/gene/269642
[3] http://www.ensembl.org/Homo_sapiens/Transcript/Summary?g=ENSG00000185818;r=4:2061239-2070815;t=ENST00000423729
[4] http://www.ensembl.org/Mus_musculus/Transcript/Summary?db=core;g=ENSMUSG00000048142;r=5:34338633-34348565;t=ENSMUST00000056355

4.2 NAT8L expression in murine tissue

qPCR analysis showed that l-NAT8L is highly expressed in brain, but also in brown adipose tissue (BAT), and to a lower extent in white adipose tissue (WAT). There was hardly any expression observed in liver samples. Interestingly, s-NAT8L was even more expressed in BAT compared to brain samples (Figure 7). l/s-NAT8L expression-pattern was not altered upon dietary interventions. Samples were taken from mice fed either a chow diet or a high-fat diet (HFD).

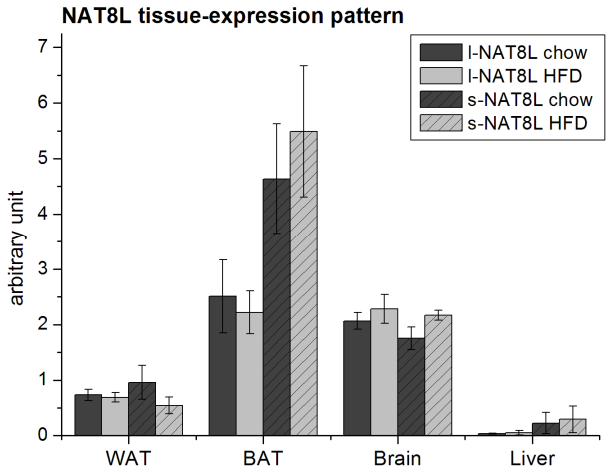

Figure 7: mRNA levels of l-NAT8L and s-NAT8L in murine WAT, BAT, brain, and liver samples from mice fed either a chow- or a high-fat diet. Results are means ± SD (n=5).

4.3 NAT8L is up-regulated during adipogenesis in human and murine cell models

qPCR analysis showed that both, the long and the short mRNA version of NAT8L, are up-regulated in different cell models during adipogenic differentiation (Figure 8, Figure 9). However, in 3T3-L1 cells, l-NAT8L was not detectable.

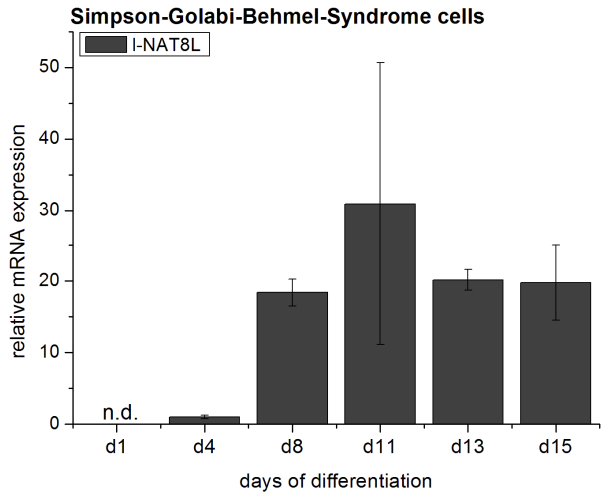

Figure 8: mRNA levels of l-NAT8L in human Simpson-Golabi-Behmel-Syndrome (SGBS-) cells during adipocenic differentiation. Data is shown as mean ±SD as the percentage of sample d4, which has been set to 1.

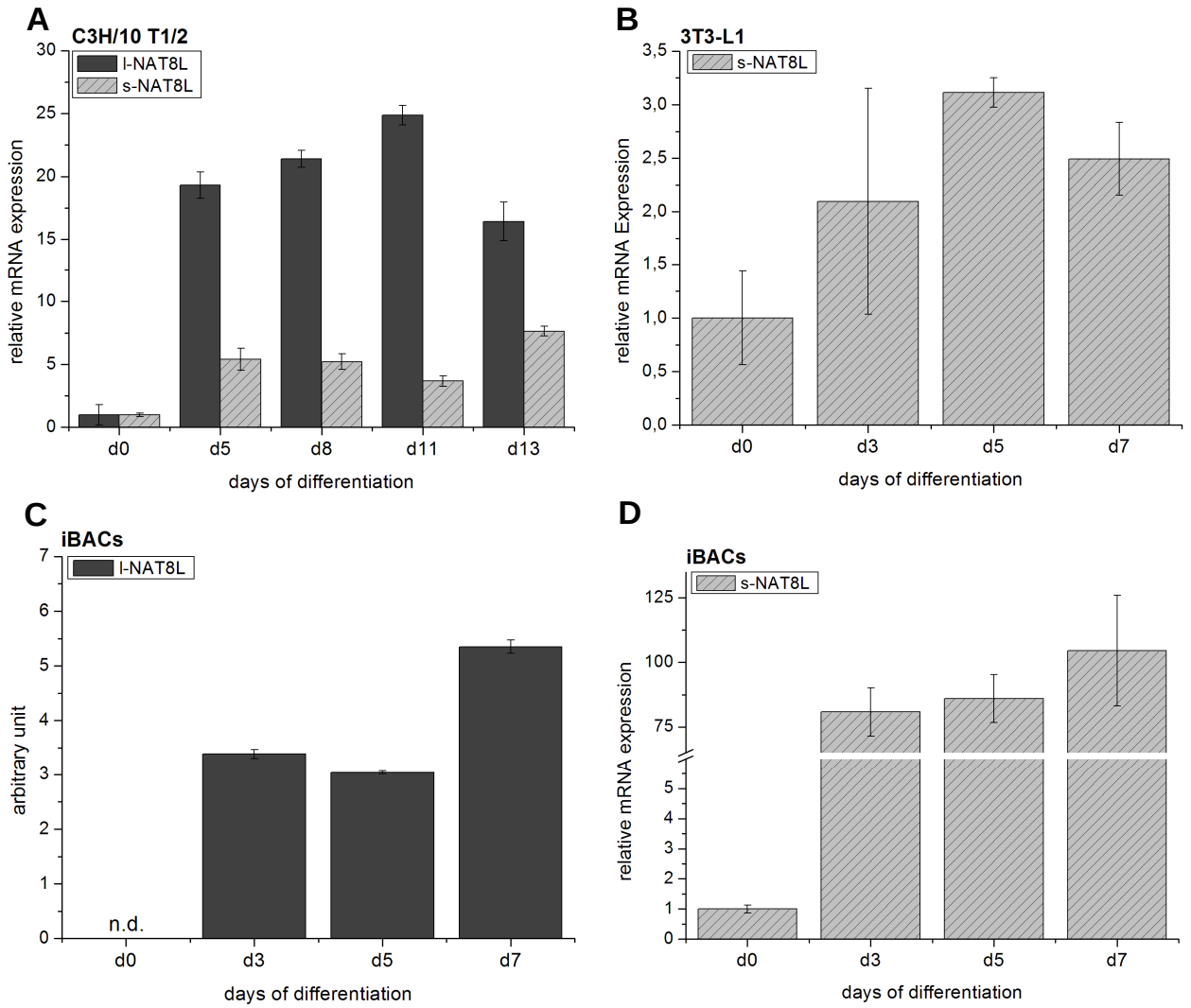

Figure 9: mRNA levels of l/s-NAT8L in different murine cell lines. (A) C3H/10 T1/2 pluripotent stem cells (B) 3T3-L1 adipocytes (C, D) iBACs. Data in all panels is shown as mean ± SD from one representative out of three biological replicates (if possible, d0 sample has been set as reference).

4.4 Characterization of iBACs using microarray analysis

To validate that iBACs are an appropriate model for brown fat differentiation *in vitro*, microarray experiments were carried out using samples of 3 independently grown and differentiated passages of iBACs. Hybridization was done with RNA collected from d3 vs. d0 cells and RNA collected from d7 vs. d0 cells. Restriction of the dataset using Genesis 1.6.0 (42) revealed a huge number of differentially expressed genes (Table 3).

Within the 4-fold cut-off dataset, some genes were found to be very likely to be up-regulated during adipogenesis per se, like ACSL1, AGPAT2, DGAT1, DGAT2, FABP4, FASN, LPL, and PPARγ.

Additionally, the DAVID “Functional Annotation Tool” (43; 44) was used to analyze the gene lists revealing “Functional Annotation Charts” (Table 4).

Table 3: Restriction and clustering results of microarray data generated with Genesis.

Restriction criteria	No. of genes	Cluster up-regulated	Cluster down-regulated
2-fold deregulated, minimum 3 values	2265	1560	705
4-fold deregulated, minimum 3 values	297	200	97

Table 4: Number of chart records (Annotation categories: GO – BP-, CC-, and MF-FAT; Pathways: BBID, BIOCARTA; KEGG_Pathways) contained in the Functional Annotation Charts generated.

Gene cluster	No. of Chart records
2-fold, minimum 3 values, up-regulated	468
2-fold, minimum 3 values, down-regulated	271

The enrichment analysis of the 2-fold down-regulated cluster did not lead to remarkable enrichment results characteristic for brown adipocytes. In contrast, enrichment analysis of the 2-fold up-regulated cluster revealed gene ontology (GO-) terms specifically characteristic for brown adipocytes (Table 5). As a representative pathway, a model of the TCA cycle and it´s adjacent biological processes underline the reliability of the dataset obtained within these experiments (Figure 10).

Table 5: Enriched terms (2-fold, minimum 3 values, up-regulated) characteristic for brown adipose tissue (KEGG …Kyoto Encyclopedia of Genes and Genomes, GO …Gene Ontology). Significance level $p<0.05$ (Benjamini-Hochberg) for all terms listed.

GO term	KEGG pathways
CC – mitochondrion	oxidative phosphorylation
CC – mitochondrial inner membrane	citrate cycle (TCA cycle)
BP – brown fat cell differentiation	PPAR signaling pathway
BP – cellular respiration	pyruvate metabolism
BP – glycolysis	fatty acid metabolism
BP – tricarboxylic acid cycle	
BP – electron transport chain	
BP – fatty acid metabolic process	

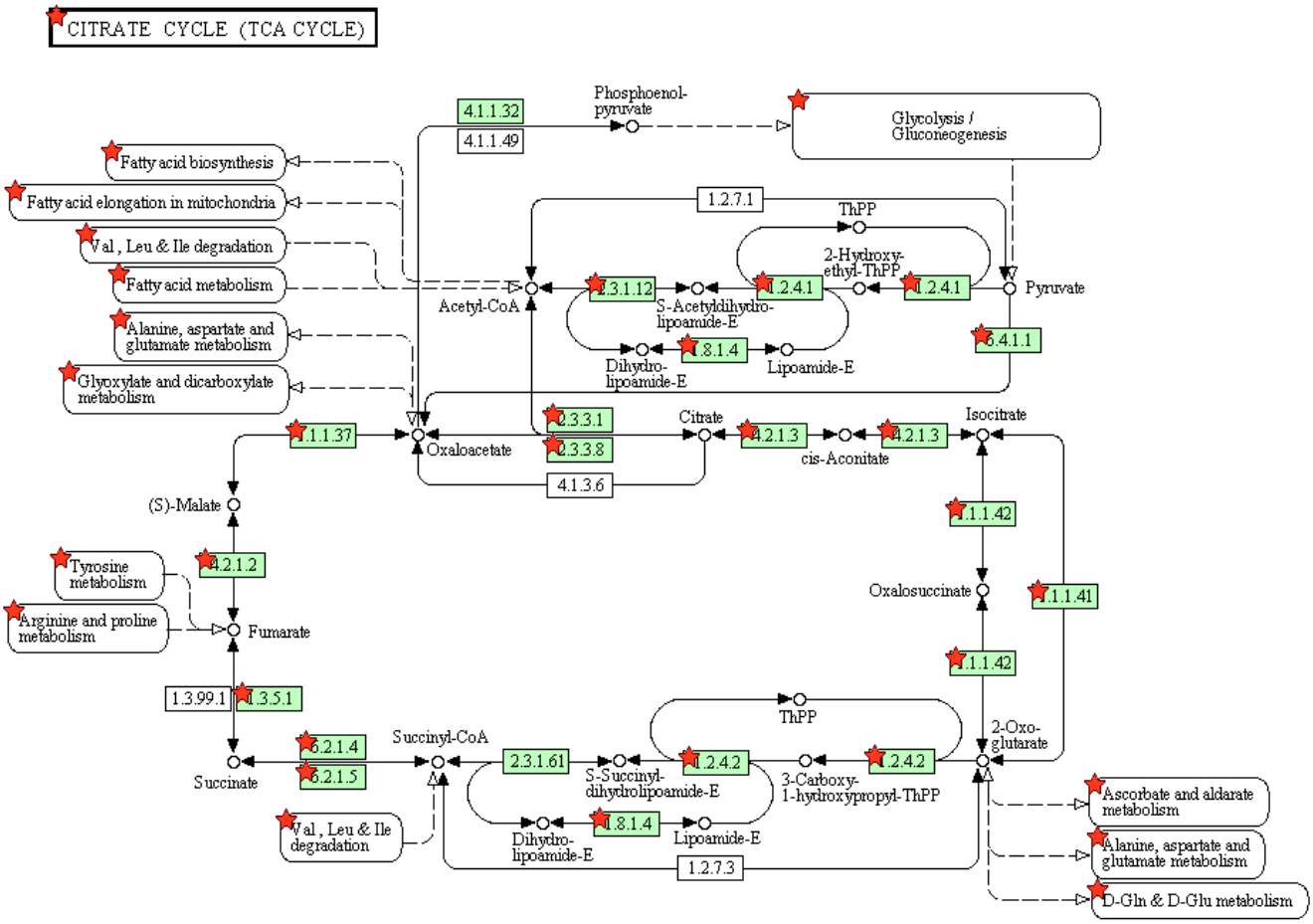

Figure 10: Kyoto Encyclopedia of Genes and Genomes (KEGG) – pathway model of the TCA cycle. Genes contained in the gene list used for enrichment analysis are indicated in light green. Significance indicated by red stars.

4.4.1 qRT-PCR and Western Blot analysis confirm µArray results

Independently of the µArray experiments, again 3 passages of iBACs were grown and differentiated. qRT-PCR was done to detect different brown fat-selective marker genes as well as general fat markers to support and validate the results obtained from µArray analysis. As expected, all these markers were highly induced during differentiation. Additionally, UCP1 expression levels could be shown with Western Blot analysis. Upon treatment with a β3-adrenergic agonist (Isoproterenol), significant induction in both mRNA and protein level of UCP1 could be observed (Figure 11).

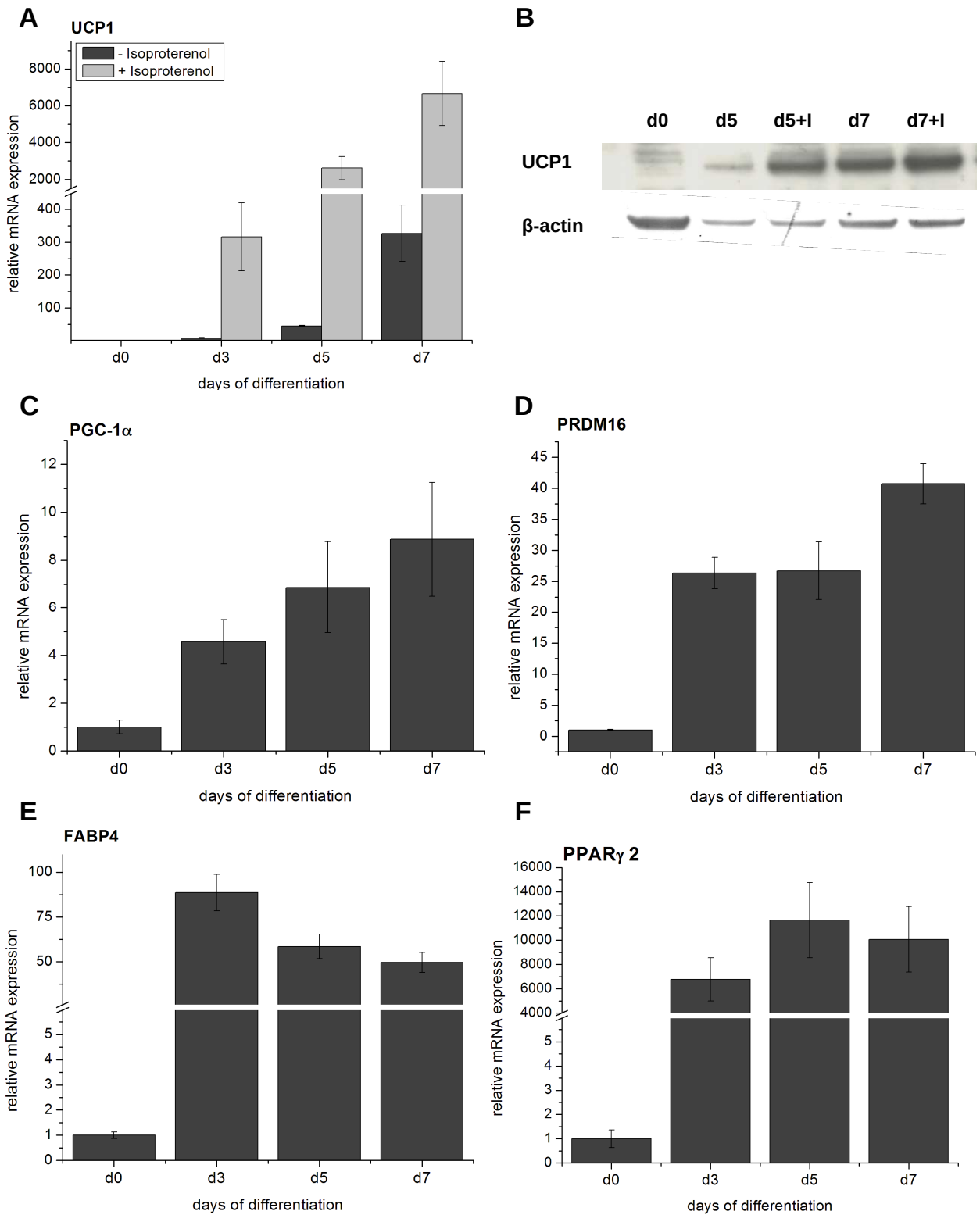

Figure 11: (A) mRNA levels of UCP1 during differentiation of iBACs (± Isoproterenol). (B) Western Blot analysis of UCP1 protein expression during differentiation (± Isoproterenol). (C-F) mRNA levels of PGC-1α, PRDM16, FABP4, and PPARγ 2 during differentiation. Data is shown from one representative replicate (n=3) as means ±SD. Sample d0 of differentiation was set to 1.

4.5 Silencing of NAT8L

As a first step to gain insight into the function of NAT8L in adipose tissue, silencing of NAT8L was evaluated in iBACs and 3T3-L1 adipocytes. For that purpose, NAT8L targeting shRNA, encoded by lentiviral vectors, was used to generate stably transduced cell lines with constitutive silencing of NAT8L expression.

4.5.1 Silencing in iBACs

As the expressions of NAT8L in BAT are comparable high as in brain, it was likely that effects in iBACs might be more significant than in 3T3-L1 cells. Two out of five different shRNA lentiviral constructs worked to silence NAT8L in iBACs. Both shRNAs target in exon 3 of the NAT8L gene, so it might be that both, l- and s-NAT8L, are affected.
As iBACs show puromycin resistance, single cells have been selected and expression levels of NAT8L have finally been determined by qRT-PCR. Silencing NAT8L in iBACs did not show an obvious phenotype. Interestingly, the two independently grown cell lines showed diverse effects on different marker genes involved in brown adipogenesis and mitochondrial biogenesis (e.g. UCP1, PPARα). Although there are big standard deviations, the silencing of l-NAT8L could be nicely shown on mRNA level (Figure 13A). Figure 13B shows western blot analysis of sil-1- compared to control-cells. On protein level, silencing could also be shown for day 1 and day 3 of differentiation for l-NAT8l (Figure 13B). Additionally, mRNA levels of s-NAT8L show a trend to be reduced upon silencing, but the effects are not that strong as for l-NAT8L (Figure 13C) and could not be verified on protein level (Figure 13B).

4.5.1.1 No differences in triglyceride (TG) accumulation upon silencing

TG content in NAT8L silenced iBACs was not altered compared to control cells (Figure 12).

4.5.1.2 Silencing of NAT8L in iBACs leads to diverse effects on brown fat-selective marker genes

To evaluate if there are any differences in expression of genes involved in brown adipogenesis or mitochondrial biogenesis, qRT-PCR analysis of different marker genes was done. The results showed different trends for the two shRNA constructs used. Since the silenced cell lines have been grown from single cells, it is possible that they show different behavior even though their developmental origin is the same. Which one of the two lines is more reliable and trustful has to be determined in further experiments (e.g. repeating the silencing). The qRT-PCR results obtained are shown in Figure 14.

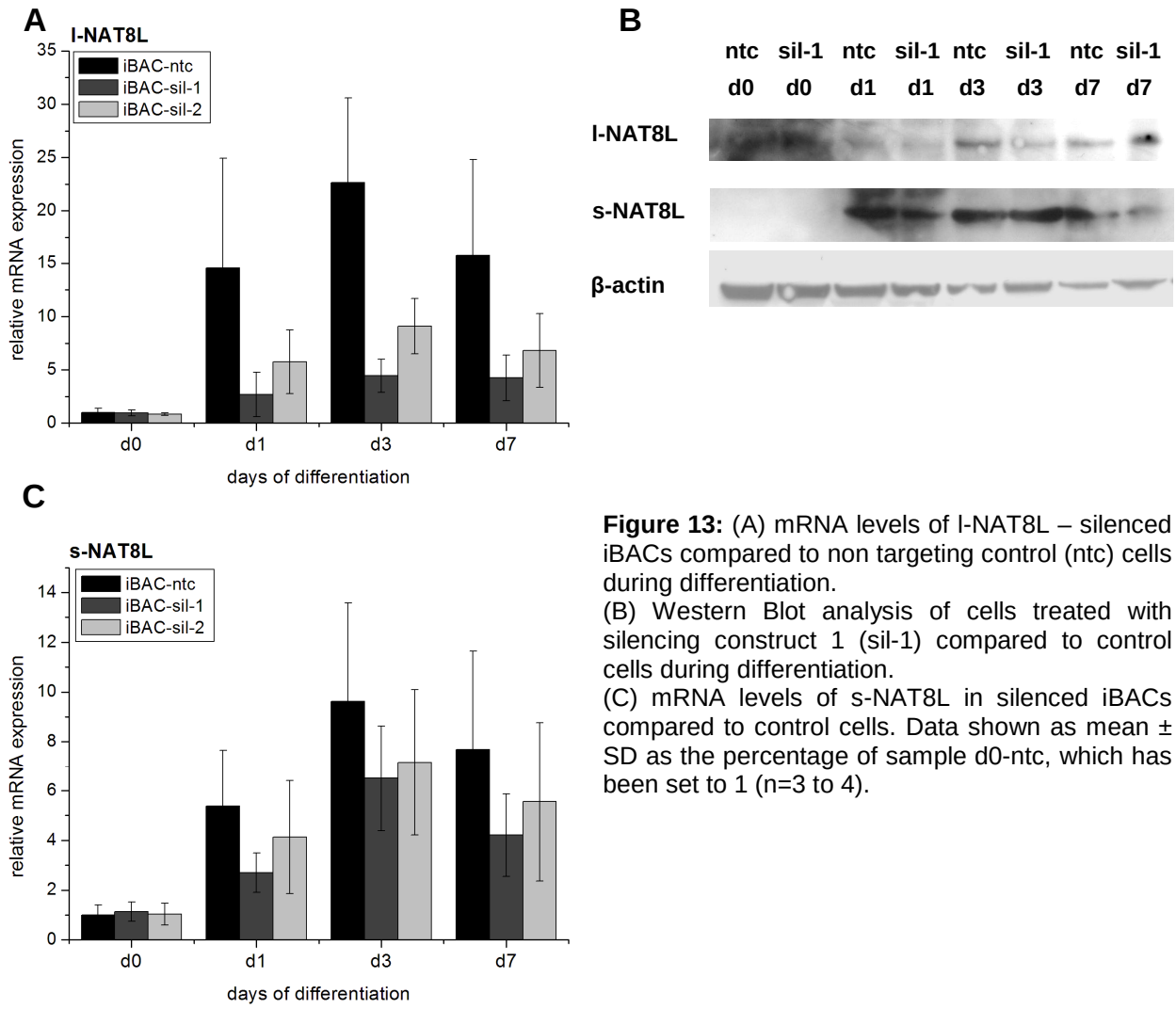

Figure 13: (A) mRNA levels of l-NAT8L – silenced iBACs compared to non targeting control (ntc) cells during differentiation.
(B) Western Blot analysis of cells treated with silencing construct 1 (sil-1) compared to control cells during differentiation.
(C) mRNA levels of s-NAT8L in silenced iBACs compared to control cells. Data shown as mean ± SD as the percentage of sample d0-ntc, which has been set to 1 (n=3 to 4).

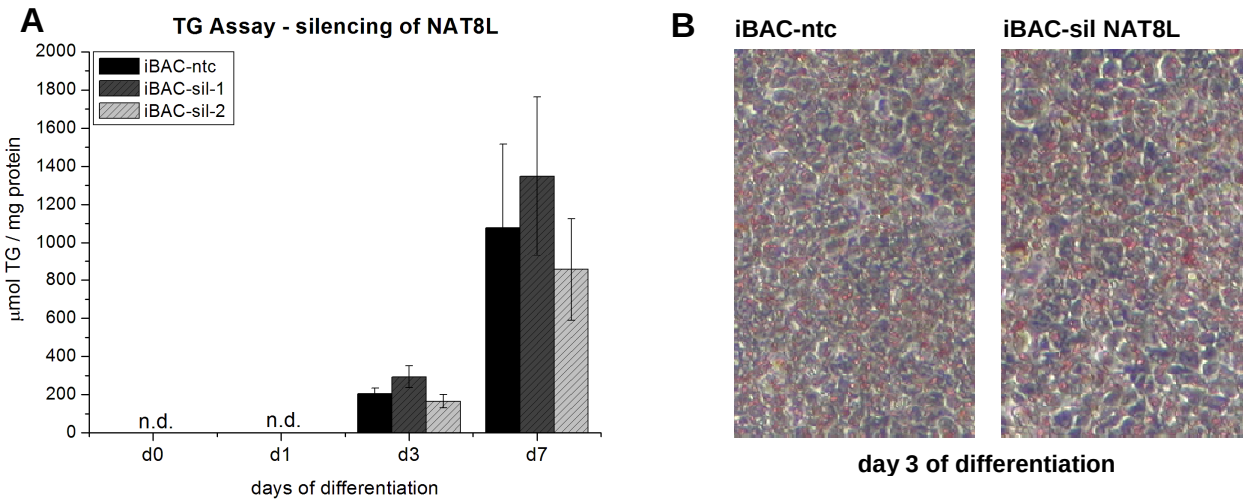

Figure 12: Triglyceride (TG) levels (A) in l-NAT8L silenced iBACs compared to control cells (iBAC-ntc). (B) Neutral lipid oil-red-o staining of iBACs on day 3 of differentiation. Data is shown as mean ± SD absolute TG in µmol TG / mg protein (n=3).

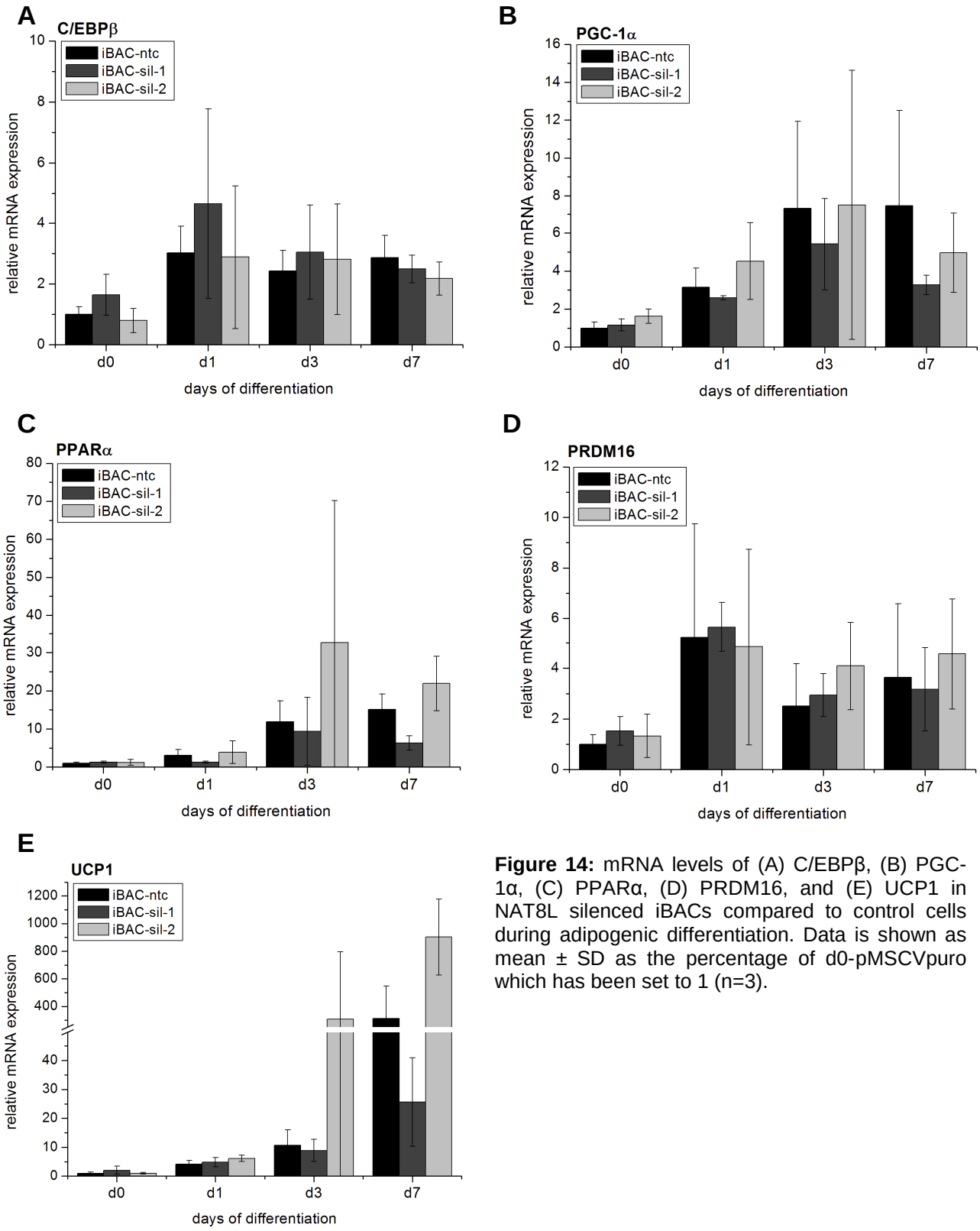

Figure 14: mRNA levels of (A) C/EBPβ, (B) PGC-1α, (C) PPARα, (D) PRDM16, and (E) UCP1 in NAT8L silenced iBACs compared to control cells during adipogenic differentiation. Data is shown as mean ± SD as the percentage of d0-pMSCVpuro which has been set to 1 (n=3).

4.5.2 Silencing in 3T3-L1 adipocytes

Silencing of NAT8L in 3T3-L1 adipocytes was done two times with the same shRNA constructs used in iBACs. For the second try, the amount of virus particles was doubled, but a significant silencing could not be reached (data not shown).

4.6 Overexpression of l-NAT8L

As silencing did not result in an obvious phenotype, the next step in elucidating the function of NAT8L in adipocytes was overexpression. For the overexpression of l-NAT8L in brown and white adipocytes, amphotrophic lentiviral particles obtained from Phoenix cells transfected with pMSCV-l-NAT8L constructs were used for transduction. Control cells were transfected with pMSCVpuro.

4.6.1 Overexpression in iBACs

As can be seen in Figure 15A, overexpression of l-NAT8L in iBACs worked well during the duration of adipogenic differentiation (up to ~100-fold). Additionally, mRNA levels of s-NAT8L seem to be induced during differentiation upon l-NAT8L overexpression compared to control cells. Overexpression of l-NAT8L could also be shown by western blot analysis even though overexpression is just obvious on day 7 of differentiation (Figure 15B and C).

4.6.1.1 Reduced lipid accumulation upon overexpression of l-NAT8L in iBACs

Overexpression of l-NAT8L in iBACs leads to a remarkable phenotypical change, namely reduced lipid accumulation. TG content was measured and seen to be significantly reduced in l-NAT8L overexpressing- compared to control cells, especially early in differentiation (day 3, see Figure 16).

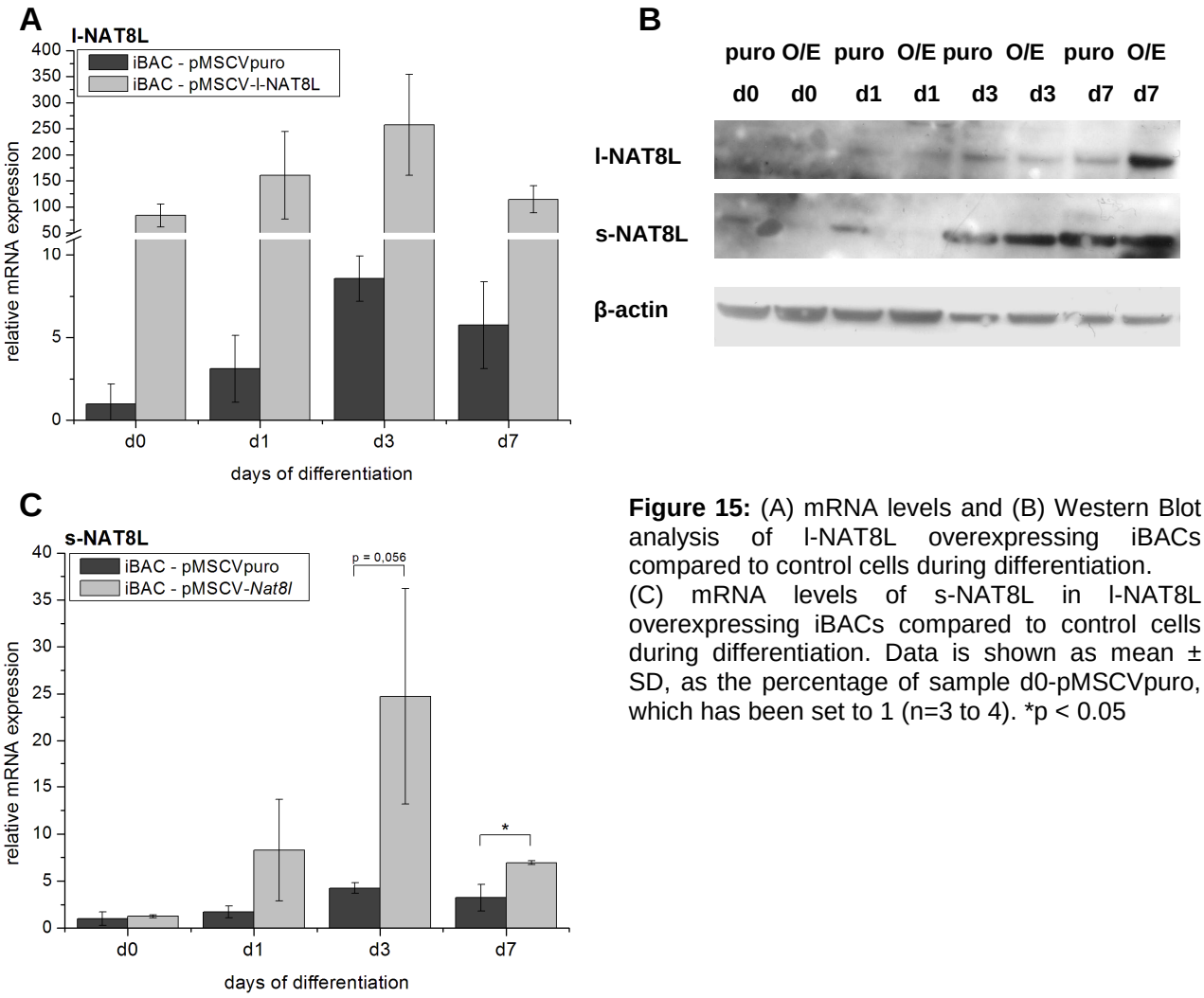

Figure 15: (A) mRNA levels and (B) Western Blot analysis of l-NAT8L overexpressing iBACs compared to control cells during differentiation. (C) mRNA levels of s-NAT8L in l-NAT8L overexpressing iBACs compared to control cells during differentiation. Data is shown as mean ± SD, as the percentage of sample d0-pMSCVpuro, which has been set to 1 (n=3 to 4). *p < 0.05

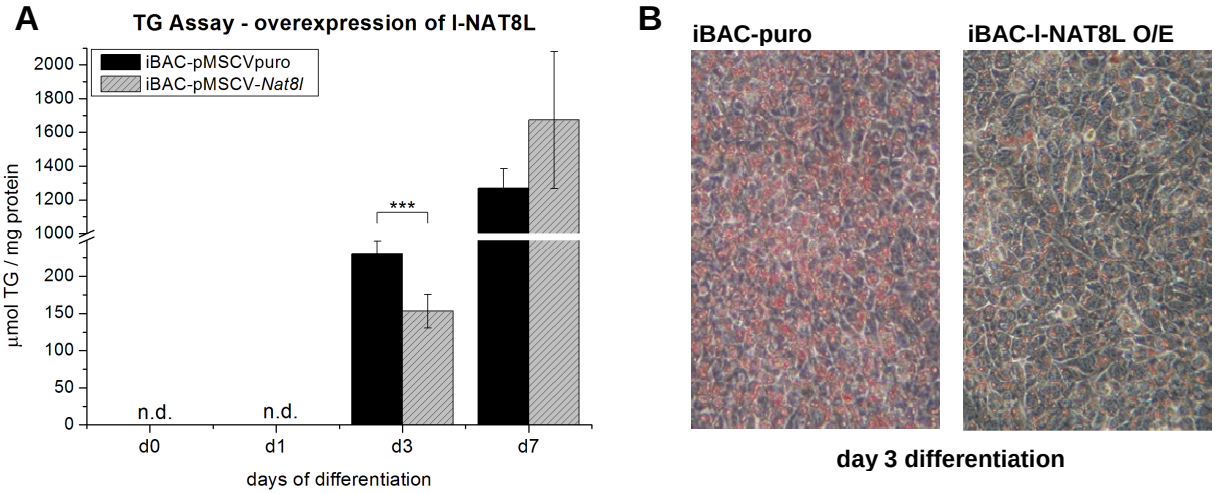

Figure 16: Triglyceride (TG) levels (A) in l-NAT8L overexpressing iBACs compared to control cells. (B) Neutral lipid oil-red-o staining of iBACs on day 3 of differentiation. Data is shown as mean ± SD absolute TG in µmol TG / mg protein (n=3). ***p < 0.001.

4.6.1.2 l-NAT8L overexpression induces various brown fat-selective marker genes in iBACs

In order to find the reason, why TG levels are reduced in iBACs that overexpress l-NAT8L, first view was taken on different marker genes involved in brown adipogenesis and mitochondrial biogenesis. qRT-PCR analysis revealed that mRNA levels of the investigated marker genes, namely C/EBPβ, PGC-1α, PPARα, PRDM16, and UCP1 were up-regulated during adipogenic differentiation in l-NAT8L overexpressing iBACs compared to control cells (Figure 18). While C/EBPβ, PGC-1α, PPARα, and PRDM16 showed increased mRNA levels throughout all days of differentiation (Figure 18A-D), transcriptional activation for UCP1 was only observed on day 7 of differentiation with an increase of ~17 fold (Figure 18E). This confers a more “brownish” phenotype to these cells.

4.6.2 Overexpression of l-NAT8L in 3T3-L1 adipocytes

To further elucidate the role of NAT8L in adipogenesis, l-NAT8L overexpressing 3T3-L1 preadipocytes and control cells (pMSCVpuro) were grown to confluence, induced to adipose differentiation 2 days after confluence, and differentiated for 8 days. RNA and TLC samples were taken on day 0, 2, 4, 6, and 8. qRT-PCR analysis showed persistent overexpression of l-NAT8L during adipogenesis (Figure 17).

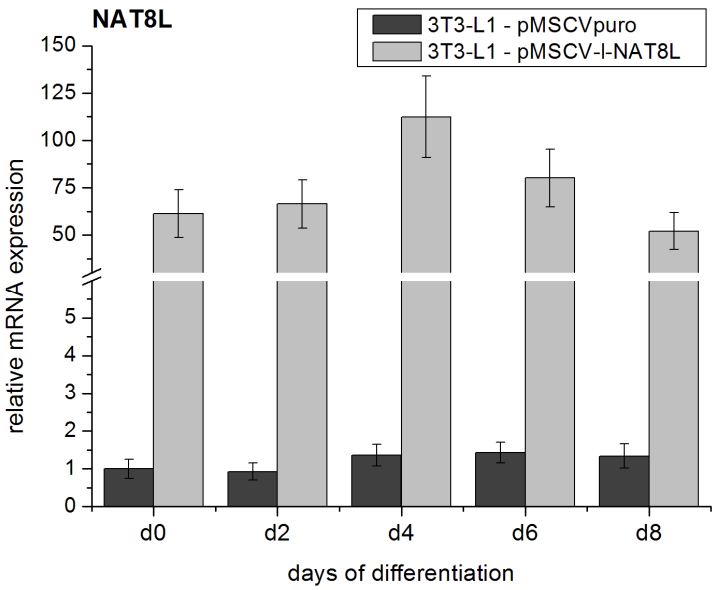

Figure 17: mRNA levels of combined l- and s-NAT8L in 3T3-L1 cells during adipogenic differentiation. Primers used detect both l- and s-NAT8L. All Data are shown as means ± SD and provided as percentage of control sample d0-pMSCVpuro, which has been set to 1. The data shown is one representative out of four biological replicates.

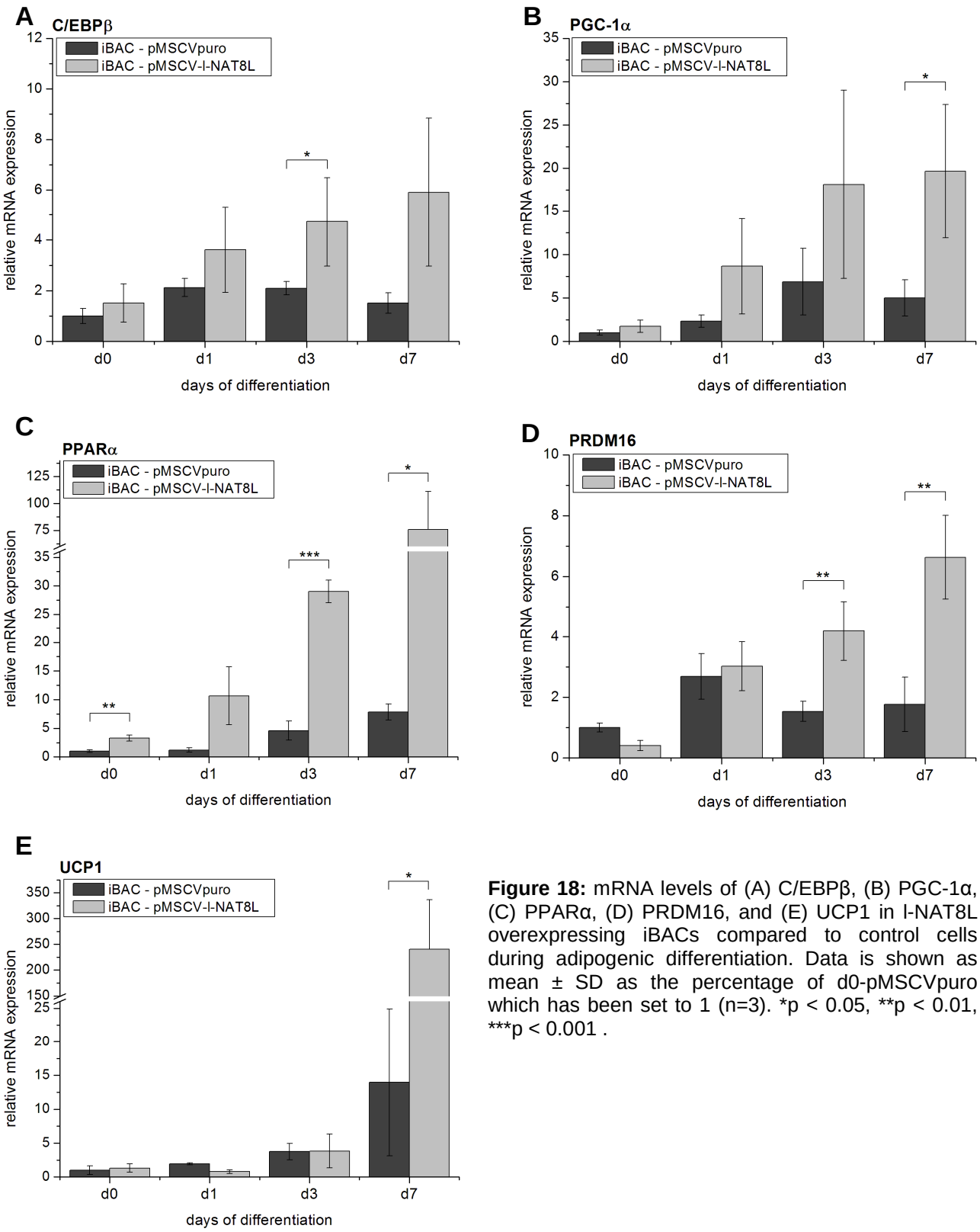

Figure 18: mRNA levels of (A) C/EBPβ, (B) PGC-1α, (C) PPARα, (D) PRDM16, and (E) UCP1 in l-NAT8L overexpressing iBACs compared to control cells during adipogenic differentiation. Data is shown as mean ± SD as the percentage of d0-pMSCVpuro which has been set to 1 (n=3). *p < 0.05, **p < 0.01, ***p < 0.001 .

Thin layer chromatography (TLC) was performed comparing control and l-NAT8L overexpression samples (Figure 19). Analysis showed that the lipid profile was unchanged in l-NAT8L overexpressing 3T3-L1 cells.

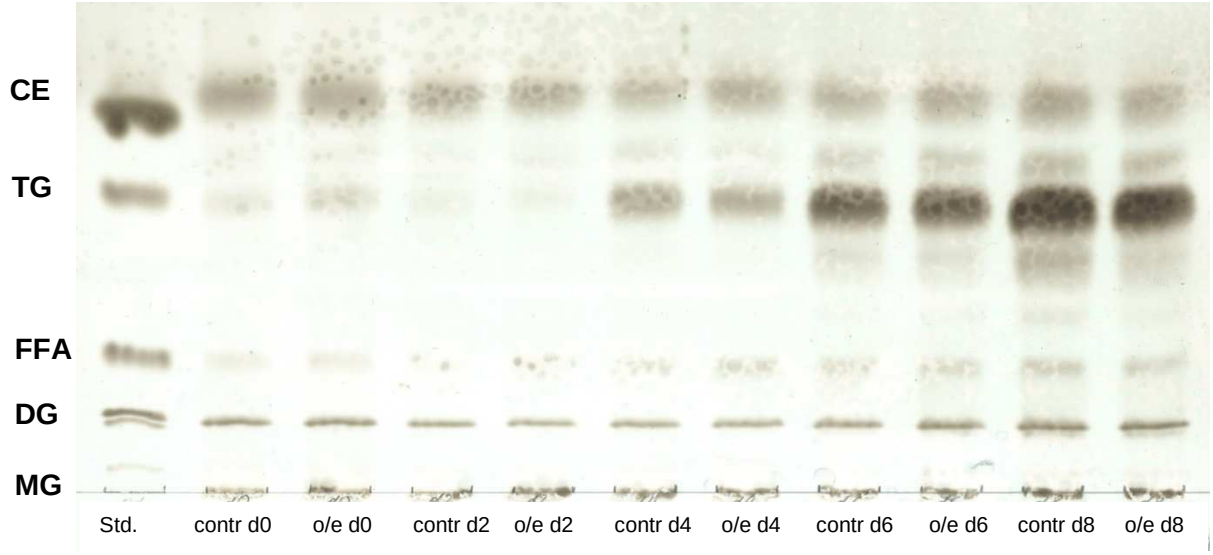

Figure 19: Thin layer chromatography comparing control and l-Nat8l overexpressing cells during adipogenic differentiation. (CE …cholesterol esters; TG …triglycerides; FFA …free fatty acids; DG …diglycerides; MG …monoglycerides)

4.6.3 No detectable "browning" effects in 3T3-L1

Since significant effects on various brown fat-specific marker genes have been observed in iBACs (see 4.6.1.2), it was obvious to have a look if this "brownish" phenotype would also occur in a white cell model. UCP1 and PRDM16 mRNA levels were not detectable in 3T3-L1 cells o/e NAT8L. However, C/EBPβ and PGC-1α mRNA levels were not altered or even reduced in comparison to control cells (Figure 20).

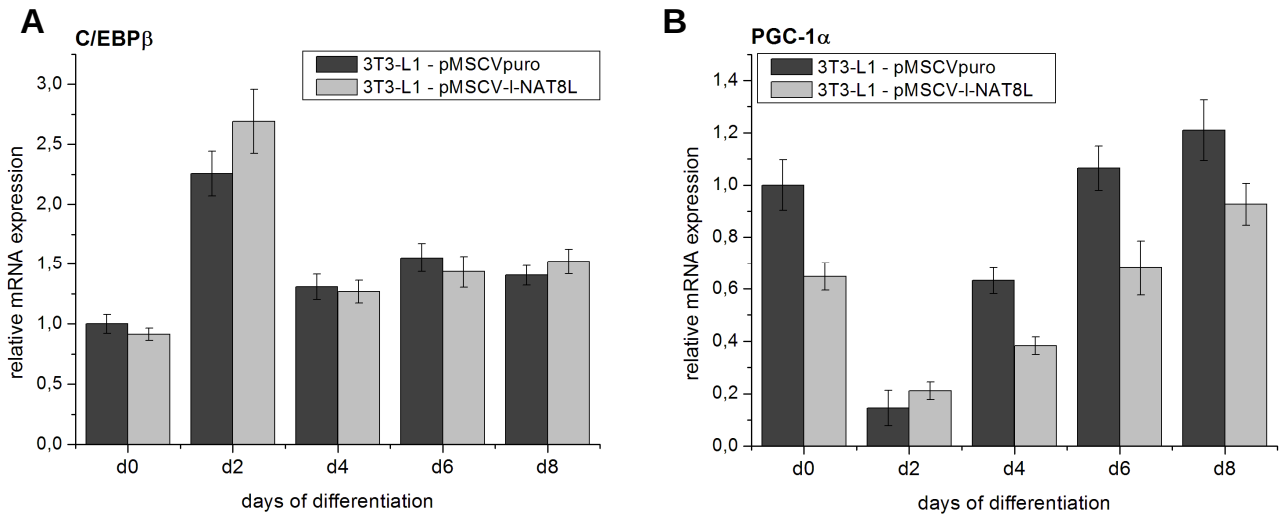

Figure 20: mRNA levels of (A) C/EBPβ and (B) PGC-1α in 3T3-L1 cells during adipogenic differentiation. Means ± SD are shown for all panels as percentage of d0-pMSCVpuro, which has been set to 1.

5 Discussion

5.1 iBACs – a novel *in vitro*-model for brown adipogenesis

As l-NAT8L expression levels are comparable in brain and BAT, it was likely to focus the experiments on brown adipose tissue. Therefore, an SV40 T-large antigen immortalized brown adipose cell line (iBACs) has been introduced to the cell culture. For the characterization of iBACs as a novel *in vitro*-model for brown adipogenesis, microarray experiments were carried out like described in 3.2.6. During differentiation of iBACs, 2,265 genes were found deregulated more than 2-fold and 297 genes even more than 4-fold, respectively (see 4.4). A look at 4-fold up-regulated genes revealed that this subset contains genes involved in adipogenesis *per se*, namely ACSL1, AGPAT2, DGAT1, DGAT2, FABP4, FASN, LPL, and PPARγ. These genes are involved e.g. in fatty acid uptake, and –esterification (45). Especially PPARγ, known as the "master-regulator" of adipogenesis, is a crucial factor for both brown and white adipogenesis (12; 13; 46; 47).
Gene enrichment analysis with a 2-fold up-regulated gene set brought up many GO-terms and pathways significantly enriched that are specific for brown adipogensis (see Table 5).
The expression levels of the major brown fat marker gene, uncoupling protein 1 (UCP1), were greatly induced on mRNA (~300-fold) and protein level comparing d7 with d0. An even higher increase could be induced upon adding a β3-adrenergic agonist (Isoproterenol) (48). Furthermore, qRT-PCR of other marker genes, namely PGC-1α, Prdm16 (13), PPARγ2, and FABP4, confirm the results obtained from microarray results (Figure 11).
All these analyses render iBACs a novel and *bona fide* model for *in vitro* differentiation of brown adipocytes beside other established cell lines (49; 50).

5.2 The role of NAT8L in brown and white adipocyte development

l-NAT8L as the NAA biosynthetic enzyme in brain and NAA as an acetyl-CoA source for lipid biosynthesis in oligodendrocytes have been reported before. Interestingly, NAA is also associated with facilitating energy metabolism in neuronal mitochondria. (2; 27–29; 31) However, implications on a role of l-NAT8L as well as NAA in adipose tissue have not been reported. Tissue screening in mice showed that beyond brain, l-NAT8L is equally expressed in BAT and to a lower extend in WAT. Additionally, a smaller protein version, s-NAT8L (see 4.1) is also expressed in brain, BAT, and WAT (Figure 7), but it has been shown, that only l- but not s-NAT8L has the N-acetyltransferase activity (2). As the human l-NAT8L protein is GCN5-related, and GCN5 is known to be a histone acetyltransferase (51), l-NAT8L might also play a role in histone acetylation and thereby transcriptional activation.
According to the tissue screening, l- and s-NAT8L mRNA levels have been measured by qRT-PCR in different cell lines (see 4.3). In both human and murine cell models, it could be shown that l- and s-NAT8L are up-regulated during adipogenic differentiation. This results

render NAT8L a possible new candidate-gene in the process of adipogenesis. Interestingly, l-NAT8L was not detectable in 3T3-L1 cells (Figure 9). Therefore, 3T3-L1 cells are an ideal system to exclusively study the effects of l-NAT8L without a basal background.

Silencing of NAT8L in iBACs was the first step in elucidating a possible function of l-NAT8L in brown adipocytes. Two different lentiviral constructs were used for silencing. Finally, a silencing rate of l-NAT8L of up to ~70% could be reached during adipogenic differentiation (Figure 13A, B). s-NAT8L showed a trend to be reduced, but not at significant levels (Figure 13C). However, an obvious phenotype could not be observed between NAT8L silenced iBACs compared to control cells, since the two cell lines derived from single cells showed different mRNA expression patterns of marker genes (Figure 14).

Stable overexpression of l-NAT8L in iBACs led to a significant changed phenotype, namely reduced lipid accumulation. Furthermore, TG measurement showed reduced TG content in l-NAT8L overexpressing compared to control cells especially on day 3 of differentiation (Figure 15, Figure 16). Additionally, qRT-PCR analysis showed significantly increased mRNA levels of brown marker genes, namely C/EBPβ, PGC-1α, PPARα, and PRDM16 (Figure 18A-D). This increase could be observed in preadipocytes (day 0 of differentiation) as well as in mature adipocytes (day 7 of differentiation). The highest increase on mRNA level could be observed for UCP1, but just on day 7 of adipogenic differentiation (~17-fold, Figure 18E). All these results confer a more “brownish” phenotype to iBACs, as all these genes are known to be crucial factors in brown fat development. PPARα has been reported to activate PGC-1α, and PGC-1α enhances mitochondrial biogenesis and expression of UCP1. PPARα has also been reported to induce PRDM16 gene expression. PRDM16 itself, together with C/EBPβ, is known to be necessary and able to induce a full brown fat- and thermogenic gene program (19; 21; 47; 52–56). All these results indicate that l-NAT8L overexpressing iBACs are in a kind of hyper-activated status. Reduced lipid accumulation upon l-NAT8L overexpression could also be shown in 3T3-L1 cells. As mentioned above, l-NAT8L has not been detectable in these cells, so it is obvious that the altered phenotype is a direct effect of l-NAT8L overexpression. However, a transcriptional activation of brown marker genes could not be observed. UCP1 and PRDM16 were not detectable, C/EBPβ and PGC-1α did not show increased mRNA levels in l-NAT8L overexpressing 3T3-L1 cells compared to controls (Figure 20). This may be explained by the fact, that 3T3-L1 cells are a classical and exclusively white fat model and activation or expression of thermogenic genes might not be possible.

With the expression patterns from l-NAT8L overexpression in iBACs, the silencing experiment can be discussed in more detail. TG levels in the cell line treated with the sil-1 construct showed a trend to be increased whereas sil-2 treated cells did not show a clear trend in TG accumulation (Figure 12A). Additionally, with qRT-PCR analysis of sil-1 treated

cells a trend to decreased mRNA levels for PGC-1α, PPARα, and UCP1 (Figure 14B, C, E) could be observed, especially late in differentiation. This would be the perfect counterpart effects observed in l-NAT8L overexpressing iBACs. However, sil-2 treated cells showed opposite effects on mRNA expression levels for the same genes. Again, it should be noted, that since the silenced cell lines have been derived from single cells (see 3.2.1.5), they might show different behavior even though their developmental origin is the same. Therefore, at least a third silenced cell line would be necessary to validate either the one or the other effect.

Within this thesis, a new transcript, s-NAT8L, could be identified for *mus musculus*. With the assumption that a 5'UTR of a shorter transcript variant of NAT8L reaches back into intron 1 of the NAT8L gene, it could be distinguished between l- and s-NAT8L by qRT-PCR analysis. However, this is not a 100% proof for a new transcript. Absolute evidence could be reached by using a 5'RACE system for rapid amplification of cDNA ends. It has been shown, that s-NAT8L protein does not possess N-acetyltransferase activity (2). Surprisingly, the mRNA levels of s-NAT8L are higher in BAT compared to brain (Figure 7), indicating a possible function in adipose tissue. Furthermore, s-NAT8L mRNA levels were increased significantly upon overexpression of l-NAT8L in iBACs. This may be a hint on a feedback regulation. However, a possible role of s-NAT8L in adipose tissue has not been reported until now and has to be determined in more detail.

In summary, the results mentioned above indicate a role of l-NAT8L in both brown and white adipogenesis. A possible model on the acting mechanism of l-NAT8L is shown in Figure 21. With one sentence, l-NAT8L overexpression may cause an imbalance between anabolic and catabolic processes within the cell. Acetyl-CoA might be much more occupied by catabolic processes like oxidative phosphorylation, the Krebs cycle, or thermogenesis (left side), leading to a decreased availability of acetyl-CoA for anabolic processes like lipid biosynthesis (right side).

However, there is still a long way to go and many questions remain unanswered. E.g. is the reduced lipid content upon l-NAT8L overexpression due to (i) a direct effect on lipid biosynthesis, (ii) an effect on cellular respiration and thermogenesis, or (iii) a metabolic effect caused by NAA? In the same breath it has to be mentioned that integration of l-NAT8L in the process of adipogenesis is highly dependent on the subcellular localization of l-NAT8L. The opinions are different, since l-NAT8L has been reported to be located in mitochondria as well as in the endoplasmic reticulum (ER) (57; 58). Fluorescence microscopy and / or cell fractionation and western blot analysis may give answers. Furthermore, the "hyperactivation of brown adipocytes" described upon l-NAT8L overexpression could be proven with oxygen consumption measurement and / or proof of increased mitochondrial number / mass within these cells. Another possibility of getting more insight on the effects of l-NAT8L on iBACs

could be transcriptome analysis with microarray experiments comparing NAT8L overexpressing cells with controls.

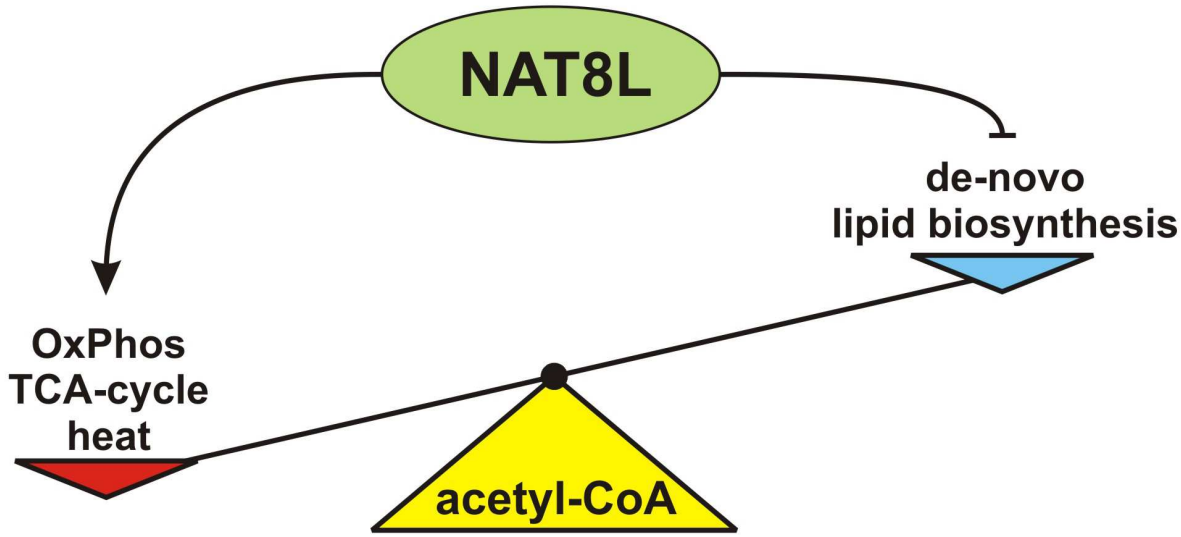

Figure 21: acetyl-CoA balance.

5.2.1 TG-measurement

TG content has been measured with protein levels as reference. The values obtained seem to be not the most reliable since protein levels varied in l-NAT8L overexpressing compared to control cells. For example, l-NAT8L o/e samples showed ~50% of the protein content measured in control cells on day 7 of differentiation. This could be effects of l-NAT8L overexpression on adipogenic differentiation. This may lead to falsified results, namely an increased measured TG content in l-NAT8L overexpressing cells compared to controls on day 7 of differentiation (Figure 16). Therefore, another / a second reference may be useful, for example the cell number. Of course, it has to be proven that the cell number is equal for the two conditions.

5.3 Concluding remarks

All in all, the results obtained in this thesis brought up many interesting facts on NAT8L. Despite the fact that many steps have to be done in the future to elucidate all the properties of this gene / protein especially in adipose tissue, it seems very promising that l-NAT8L has significant effects on brown fat differentiation and thermogenic activity. Therefore, l-NAT8L may provide a new possibility to increase energy expenditure and thereby finding new therapeutic ways for the treatment, but also the prevention of obesity.

6 Figure Legends

6 Figure Legends

7 References

7 References

1. Pinent M, Hackl H, Burkard TR, Prokesch A, Papak C, Scheideler M, Hämmerle G, Zechner R, Trajanoski Z, Strauss JG. Differential transcriptional modulation of biological processes in adipocyte triglyceride lipase and hormone-sensitive lipase-deficient mice. Genomics 2008 Jul;92(1):26-32.[cited 2012 Jan 26]
2. Wiame E, Tyteca D, Pierrot N, Collard F, Amyere M, Noel G, Desmedt J, Nassogne M-C, Vikkula M, Octave J-N, Vincent M-F, Courtoy PJ, Boltshauser E, van Schaftingen E. Molecular identification of aspartate N-acetyltransferase and its mutation in hypoacetylaspartia. Biochem. J. 2010 Jan;425(1):127-136.[cited 2012 Jan 23]
3. Tipton CM. Susruta of India, an unrecognized contributor to the history of exercise physiology. Journal of Applied Physiology 2008 Jun;104(6):1553 -1556.[cited 2012 Jan 25]
4. Ferris WF, Crowther NJ. Once fat was fat and that was that: our changing perspectives on adipose tissue. Cardiovasc J Afr 2011 Jun;22(3):147-154.[cited 2012 Jan 2]
5. Ahima RS. Digging deeper into obesity. J. Clin. Invest. 2011 Jun;121(6):2076-2079.[cited 2012 Jan 25]
6. Finucane MM, Stevens GA, Cowan MJ, Danaei G, Lin JK, Paciorek CJ, Singh GM, Gutierrez HR, Lu Y, Bahalim AN, Farzadfar F, Riley LM, Ezzati M. National, regional, and global trends in body-mass index since 1980: systematic analysis of health examination surveys and epidemiological studies with 960 country-years and 9·1 million participants. Lancet 2011 Feb;377(9765):557-567.[cited 2012 Jan 25]
7. Spiegelman BM, Flier JS. Obesity and the regulation of energy balance. Cell 2001 Feb;104(4):531-543.[cited 2012 Jan 25]
8. Richard D, Picard F. Brown fat biology and thermogenesis. Front. Biosci. 2011;16:1233-1260.[cited 2012 Jan 26]
9. Yao X, Shan S, Zhang Y, Ying H. Recent progress in the study of brown adipose tissue. Cell Biosci 2011;1:35.[cited 2012 Jan 2]
10. CANNON B, NEDERGAARD J. Brown Adipose Tissue: Function and Physiological Significance. Physiological Reviews 2004 Jan;84(1):277 -359.[cited 2011 Oct 28]
11. Nedergaard J, Bengtsson T, Cannon B. Unexpected evidence for active brown adipose tissue in adult humans. Am. J. Physiol. Endocrinol. Metab. 2007 Aug;293(2):E444-452.[cited 2012 Jan 26]
12. Farmer SR. Transcriptional control of adipocyte formation. Cell Metab. 2006 Oct;4(4):263-273.[cited 2012 Jan 26]
13. Seale P. Transcriptional control of brown adipocyte development and thermogenesis. Int J Obes (Lond) 2010 Oct;34 Suppl 1:S17-22.[cited 2012 Jan 26]
14. Rosen ED, MacDougald OA. Adipocyte differentiation from the inside out. Nat. Rev. Mol. Cell Biol. 2006 Dec;7(12):885-896.[cited 2012 Jan 26]
15. Schulz TJ, Huang TL, Tran TT, Zhang H, Townsend KL, Shadrach JL, Cerletti M, McDougall LE, Giorgadze N, Tchkonia T, Schrier D, Falb D, Kirkland JL, Wagers AJ, Tseng Y-H. Identification of inducible brown adipocyte progenitors residing in skeletal muscle and white fat. Proc. Natl. Acad. Sci. U.S.A. 2011 Jan;108(1):143-148.[cited 2012 Jan 26]
16. Timmons JA, Wennmalm K, Larsson O, Walden TB, Lassmann T, Petrovic N, Hamilton DL, Gimeno RE, Wahlestedt C, Baar K, Nedergaard J, Cannon B. Myogenic gene expression signature establishes that brown and white adipocytes originate from distinct cell lineages. Proc. Natl. Acad. Sci. U.S.A. 2007 Mar;104(11):4401-4406.[cited 2012 Jan 26]
17. Ishibashi J, Seale P. Beige can be slimming. Science 2010 May;328(5982):1113-1114.
18. Svensson P-A, Jernås M, Sjöholm K, Hoffmann JM, Nilsson BE, Hansson M, Carlsson LMS. Gene expression in human brown adipose tissue. Int. J. Mol. Med. 2011 Feb;27(2):227-232.[cited 2012 Jan 26]
19. Seale P, Bjork B, Yang W, Kajimura S, Chin S, Kuang S, Scimè A, Devarakonda S, Conroe HM, Erdjument-Bromage H, Tempst P, Rudnicki MA, Beier DR, Spiegelman BM. PRDM16 controls a brown fat/skeletal muscle switch. Nature 2008 Aug;454(7207):961-967.[cited 2012 Jan 26]
20. Uldry M, Yang W, St-Pierre J, Lin J, Seale P, Spiegelman BM. Complementary action of the PGC-1 coactivators in mitochondrial biogenesis and brown fat differentiation. Cell Metab. 2006 May;3(5):333-341.[cited 2011 Oct 28]
21. Carmona MC, Hondares E, Rodríguez de la Concepción ML, Rodríguez-Sureda V, Peinado-Onsurbe J, Poli V, Iglesias R, Villarroya F, Giralt M. Defective thermoregulation, impaired lipid metabolism, but preserved adrenergic induction of gene expression in brown fat of mice lacking C/EBPbeta. Biochem. J. 2005 Jul;389(Pt 1):47-56.[cited 2011 Oct 28]
22. Cannon B, Nedergaard J. Nonshivering thermogenesis and its adequate measurement in metabolic studies. J. Exp. Biol. 2011 Jan;214(Pt 2):242-253.[cited 2012 Jan 26]
23. Seale P, Lazar MA. Brown fat in humans: turning up the heat on obesity. Diabetes 2009 Jul;58(7):1482-1484.[cited 2012 Jan 26]
24. Tews D, Wabitsch M. Renaissance of brown adipose tissue. Horm Res Paediatr 2011;75(4):231-239.[cited 2012 Jan 26]
25. Kajimura S, Seale P, Spiegelman BM. Transcriptional control of brown fat development. Cell Metab. 2010 Apr;11(4):257-262.[cited 2012 Jan 26]
26. Himms-Hagen J, Melnyk A, Zingaretti MC, Ceresi E, Barbatelli G, Cinti S. Multilocular fat cells in WAT of CL-316243-treated rats derive directly from white adipocytes. Am. J. Physiol., Cell Physiol. 2000 Sep;279(3):C670-681.[cited 2012 Jan 26]
27. Ariyannur PS, Moffett JR, Manickam P,

Pattabiraman N, Arun P, Nitta A, Nabeshima T, Madhavarao CN, Namboodiri AMA. Methamphetamine-induced neuronal protein NAT8L is the NAA biosynthetic enzyme: implications for specialized acetyl coenzyme A metabolism in the CNS. Brain Res. 2010 Jun;1335:1-13.[cited 2012 Jan 28]

28. Chakraborty G, Mekala P, Yahya D, Wu G, Ledeen RW. Intraneuronal N-acetylaspartate supplies acetyl groups for myelin lipid synthesis: evidence for myelin-associated aspartoacylase. J. Neurochem. 2001 Aug;78(4):736-745.[cited 2012 Jan 28]
29. Mehta V, Namboodiri MA. N-acetylaspartate as an acetyl source in the nervous system. Brain Res. Mol. Brain Res. 1995 Jul;31(1-2):151-157.[cited 2012 Jan 28]
30. Baslow MH. N-acetylaspartate in the vertebrate brain: metabolism and function. Neurochem. Res. 2003 Jun;28(6):941-953.[cited 2012 Jan 23]
31. Burri R, Steffen C, Herschkowitz N. N-acetyl-L-aspartate is a major source of acetyl groups for lipid synthesis during rat brain development. Dev. Neurosci. 1991;13(6):403-411.[cited 2012 Jan 28]
32. Moffett JR, Ross B, Arun P, Madhavarao CN, Namboodiri AMA. N-Acetylaspartate in the CNS: from neurodiagnostics to neurobiology. Prog. Neurobiol. 2007 Feb;81(2):89-131.[cited 2012 Jan 28]
33. Green H, Meuth M. An established pre-adipose cell line and its differentiation in culture. Cell 1974 Oct;3(2):127-133.[cited 2012 Jan 24]
34. Green H, Kehinde O. Spontaneous heritable changes leading to increased adipose conversion in 3T3 cells. Cell 1976 Jan;7(1):105-113.[cited 2012 Jan 24]
35. Tang Q-Q, Otto TC, Lane MD. Commitment of C3H10T1/2 pluripotent stem cells to the adipocyte lineage. Proc. Natl. Acad. Sci. U.S.A. 2004 Jun;101(26):9607-9611.[cited 2012 Jan 24]
36. Huang H, Song T-J, Li X, Hu L, He Q, Liu M, Lane MD, Tang Q-Q. BMP signaling pathway is required for commitment of C3H10T1/2 pluripotent stem cells to the adipocyte lineage. Proc. Natl. Acad. Sci. U.S.A. 2009 Aug;106(31):12670-12675.[cited 2012 Jan 24]
37. Wabitsch M, Brenner RE, Melzner I, Braun M, Möller P, Heinze E, Debatin KM, Hauner H. Characterization of a human preadipocyte cell strain with high capacity for adipose differentiation. Int. J. Obes. Relat. Metab. Disord. 2001 Jan;25(1):8-15.[cited 2012 Jan 24]
38. Fischer-Posovszky P, Newell FS, Wabitsch M, Tornqvist HE. Human SGBS cells - a unique tool for studies of human fat cell biology. Obes Facts 2008;1(4):184-189.[cited 2012 Jan 24]
39. Leung YF, Cavalieri D. Fundamentals of cDNA microarray data analysis. Trends Genet. 2003 Nov;19(11):649-659.[cited 2012 Jan 24]
40. Quackenbush J. Computational analysis of microarray data. Nat. Rev. Genet. 2001 Jun;2(6):418-427.[cited 2012 Jan 24]
41. Rainer J, Sanchez-Cabo F, Stocker G, Sturn A, Trajanoski Z. CARMAweb: comprehensive R- and bioconductor-based web service for microarray data analysis. Nucleic Acids Res. 2006 Jul;34(Web Server issue):W498-503.[cited 2012 Jan 16]
42. Sturn A, Quackenbush J, Trajanoski Z. Genesis: cluster analysis of microarray data. Bioinformatics 2002 Jan;18(1):207-208.[cited 2012 Jan 16]
43. Huang DW, Sherman BT, Lempicki RA. Bioinformatics enrichment tools: paths toward the comprehensive functional analysis of large gene lists. Nucleic Acids Res. 2009 Jan;37(1):1-13.[cited 2012 Jan 13]
44. Huang DW, Sherman BT, Lempicki RA. Systematic and integrative analysis of large gene lists using DAVID bioinformatics resources. Nat Protoc 2009;4(1):44-57.[cited 2012 Jan 13]
45. Clément K. Novel Insights Into Adipose Cell Functions. Springer; 2010.
46. Rosen ED, Spiegelman BM. Molecular regulation of adipogenesis. Annu. Rev. Cell Dev. Biol. 2000;16:145-171.[cited 2012 Feb 4]
47. Villarroya F, Iglesias R, Giralt M. PPARs in the Control of Uncoupling Proteins Gene Expression. PPAR Research 2007;2007:1-12.[cited 2012 Jan 13]
48. Bengtsson T, Cannon B, Nedergaard J. Differential adrenergic regulation of the gene expression of the beta-adrenoceptor subtypes beta1, beta2 and beta3 in brown adipocytes. Biochem. J. 2000 May;347 Pt 3:643-651.[cited 2012 Feb 4]
49. Klein J, Fasshauer M, Klein HH, Benito M, Kahn CR. Novel adipocyte lines from brown fat: a model system for the study of differentiation, energy metabolism, and insulin action. Bioessays 2002 Apr;24(4):382-388.[cited 2012 Feb 4]
50. Klaus S, Choy L, Champigny O, Cassard-Doulcier AM, Ross S, Spiegelman B, Ricquier D. Characterization of the novel brown adipocyte cell line HIB 1B. Adrenergic pathways involved in regulation of uncoupling protein gene expression. J. Cell. Sci. 1994 Jan;107 (Pt 1):313-319.[cited 2012 Feb 4]
51. Dyda F, Klein DC, Hickman AB. GCN5-related N-acetyltransferases: a structural overview. Annu Rev Biophys Biomol Struct 2000;29:81-103.[cited 2012 Feb 4]
52. Hondares E, Rosell M, Díaz-Delfín J, Olmos Y, Monsalve M, Iglesias R, Villarroya F, Giralt M. Peroxisome proliferator-activated receptor α (PPARα) induces PPARγ coactivator 1α (PGC-1α) gene expression and contributes to thermogenic activation of brown fat: involvement of PRDM16. J. Biol. Chem. 2011 Dec;286(50):43112-43122.[cited 2012 Feb 5]
53. Seale P, Conroe HM, Estall J, Kajimura S, Frontini A, Ishibashi J, Cohen P, Cinti S, Spiegelman BM. Prdm16 determines the thermogenic program of subcutaneous white adipose tissue in mice. J. Clin. Invest. 2011

Jan;121(1):96-105.[cited 2012 Feb 5]
54. Seale P, Kajimura S, Yang W, Chin S, Rohas LM, Uldry M, Tavernier G, Langin D, Spiegelman BM. Transcriptional control of brown fat determination by PRDM16. Cell Metab. 2007 Jul;6(1):38-54.[cited 2012 Feb 5]
55. Kajimura S, Seale P, Kubota K, Lunsford E, Frangioni JV, Gygi SP, Spiegelman BM. Initiation of myoblast to brown fat switch by a PRDM16-C/EBP-beta transcriptional complex. Nature 2009 Aug;460(7259):1154-1158.[cited 2012 Feb 5]
56. Huang P-I, Chen Y-C, Chen L-H, Juan C-C, Ku H-H, Wang S-T, Chiou S-H, Chiou G-Y, Chi C-W, Hsu C-C, Lee H-C, Chen L-K, Kao C-L. PGC-1α mediates differentiation of mesenchymal stem cells to brown adipose cells. J. Atheroscler. Thromb. 2011;18(11):966-980.[cited 2012 Feb 5]
57. Tahay G, Wiame E, Tyteca D, Courtoy PJ, Van Schaftingen E. Determinants of the enzymatic activity and the subcellular localization of aspartate N-acetyltransferase. Biochem. J. 2012 Jan;441(1):105-112.[cited 2012 Feb 4]
58. Arun P, Moffett JR, Namboodiri AMA. Evidence for mitochondrial and cytoplasmic N-acetylaspartate synthesis in SH-SY5Y neuroblastoma cells. Neurochem. Int. 2009 Sep;55(4):219-225.[cited 2012 Feb 4]